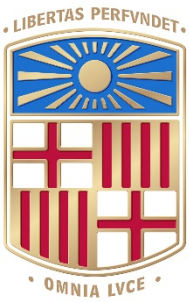


UNIVERSITAT DE BARCELONA

Final Degree Project

**Biomedical Engineering Degree**

# Localization of sources in electroencephalographic registers during working memory tasks.

Barcelona, 21 de juny de 2021

Author: Ana Cordón Avila

Director/s: Albert Compte

Tutor: Santiago Marco

## ACKNOWLEDGMENTS

I would like to thank Albert Compte for giving me the opportunity to perform my final degree project on computational neuroscience. Also, I would like to thank all my friends and fellow biomedical engineers whom I have shared these four years of hard work and remarkable experiences. Finally, I would like to express my gratitude to my family for their unconditional support.

## ABSTRACT

EEG source localization is a non-invasive imaging technique developed to locate the anatomical sources recorded at the scalp during an EEG recording. The reconstruction of the sources can be computed by solving the so-called inverse problem. This is an ill-posed problem which aims in estimating the sources that fit the recorded measurements. There exist several powerful commercial and academic software packages that cover multiple methods on data processing, source localization, and statistical analysis.

In this work, the open-source MNE-Python package was selected as the working environment used to address the challenge of characterizing and locating neural activation. This study provides a pipeline with practical steps on the EEG source localization technique. The results obtained in this project have been validated by experts in the Theoretical Neurobiology and Computational Neuroscience fields

In this project, the EEG source localization has been computed over a group of encephalitic patients and a control group. The two groups had shown differences regarding the electrical activity in a working memory trial. This study aimed in localizing the anatomical brain regions that were responsible of the electrical differences. It has been observed that instants before the stimulus, the activated sites between control groups and encephalitic groups differ. In the case of the control group, the activated region was located at the frontal lobe of the left hemisphere. Whereas, in the case of the encephalitic group the activated region was located at the temporal lobe of the right hemisphere.

### KEYWORDS

Electroencephalography · magnetic resonance imaging · source reconstruction · inverse problem · forward problem · boundary element model · source space

**TABLE OF CONTENTS**

ACKNOWLEDGMENTS ..... I

ABSTRACT ..... II

LIST OF FIGURES ..... V

LIST OF TABLES ..... VI

GLOSSARY OF TERMS ..... VII

1. INTRODUCTION ..... 1

1.1. Objectives ..... 2

1.2. Methods and structure of the project ..... 3

1.3. Scope ..... 4

1.4 Location of the project ..... 5

2. BACKGROUND ..... 6

2.1. State-of-the-art ..... 6
2.1.1. EEG ..... 6
2.1.2 Anatomical modelling ..... 8
2.1.3. Inverse Problem ..... 10
2.1.4. Inverse solutions ..... 11

2.3. State of the situation ..... 12

3. MARKET ANALYSIS ..... 14

3.1. Sectors to which it is directed ..... 14

3.2. Historical evolution of the market and future market prospects ..... 14

3.3. Product environment ..... 16

4. CONCEPTION DESIGN ..... 17

4.1. Solutions study ..... 17
4.1.1. Solution 1: MNE-Python ..... 17
4.1.2. Solution 2: FieldTrip ..... 18
4.1.3. Solution 3: Brainstorm ..... 19

4.1.4. Summary of possible solutions ..... 19

4.2. Proposed solution ..... 20

5. DETAILED ENGINEERING ..... 21

5.1. Initial data ..... 21
5.1.1. Experimental sample ..... 21
5.1.2. Trial description – memory task ..... 22
5.1.3. Processing EEG data ..... 22
5.1.4. Anatomical Sample ..... 23

5.2. Pipeline implemented ..... 23
5.2.1. Installation ..... 23
5.2.2. Reconstruction anatomical MRI using FreeSurfer ..... 24
5.2.3. Processing EEG data ..... 24
5.2.4. Forward operator ..... 25
5.2.5. Inverse Solution ..... 28

5.3. Results ..... 28
5.3.1. Method selected ..... 29
5.3.2. Model validation ..... 29
5.3.3. Final Results ..... 31
5.3.4. Discussion ..... 33

6. EXECUTION PLAN ..... 35

7. TECHNICAL FEASIBILITY ..... 36

8. ECONOMICAL FEASIBILITY ..... 37

9. REGULATION AND LEGAL ASPECTS ..... 39

10. CONCLUSIONS AND FUTURE LINES ..... 40

11. REFERENCES ..... 41

12. ANNEXES ..... 45

12.1. FreeSurfer – Anatomical MRI reconstruction ..... 45

12.2. FreeSurfer – BEM model ..... 45

12.3. PCA analysis results ..... 45

12.4. PCA analysis code ..... 46

12.5. Source Reconstruction code ..... 51

## LIST OF FIGURES

**Figure 1**: EEG recording [47] ..... 1
**Figure 2**: Enobio 8 by Neuroelectrics [49] ..... 7
**Figure 3**: Electrode Montage [50] ..... 8
**Figure 4**: Example mesh of the human head used in BEM; triangulated surfaces of the brain, skull and scalp compartments [20] ..... 10
**Figure 5**: An illustration of the forward and inverse problems in the context of EEG [22] ..... 10
**Figure 6**: Functional architecture of a typical BCI [11] ..... 15
**Figure 7**: Example of a MEG equipment [51] ..... 16
**Figure 8**: Trial illustration ..... 22
**Figure 9 and 10**: Noise covariance matrix and evoked data. ..... 25
**Figure 11**: Surfaces segmented by FreeSurfer ..... 26
**Figure 12 and 13**: Surface-based source space example ..... 27
**Figure 14**: Workflow of the MNE software.[6] ..... 28
**Figure 15**: Brain lobes [61] ..... 30
**Figures 16 and 17**: 16 represents the longepoch result (t=0s) and 17 represents the respeoch results (t=0s) ..... 31
**Figure 18 and 19**: 18 and 19 depict the first two PCs and considered clusters for the source coordinates of the left and right hemispheres in Control and Encephalitic Group, respectively ..... 32
**Figure 20 and 21**: Control 4 and encephalitic 7 sources of activation at time -0.9s. ..... 33
**Figure 22**: GANTT graph of the project ..... 35
**Figure 23 and 24**: 23 and 24 depict the first two PCs and considered clusters for the source coordinates of the right and left hemispheres in Control and Encephalitic Group, respectively ..... 46

## LIST OF TABLES

TABLE 1: SOFTWARE PACKAGES AVAILABLE ONLINE TO SOLVE THE INVERSE PROBLEM .....13

TABLE 2: STUDIED SOLUTIONS.....17

TABLE 3: SUMMARY OF SOFTWARE FEATURES [34] .....20

TABLE 4: MEAN AND STANDARD DEVIATION OF THE LOCALIZED SOURCES IN CONTROL AND ENCEPHALITIC GROUPS. .....32

TABLE 5: COST AND TIME REQUIRED FOR AN MRI AND EEG EXAM .....37

TABLE 6: COST OF DATA ACQUISITION AND COST FOR EACH GROUP.....37

TABLE 7 TECHNICIANS AND EQUIPMENT BUDGET.....37

## GLOSSARY OF TERMS

**ADHD**: Attention-deficit/hyperactivity disorder
**Anti-NMAR Encephalitis**: Anti-N-methyl-D-aspartate receptor encephalitis
**BCI**: Brain computer interface
**BEM**: Boundary element method
**CT**: Computerized tomography
**dSPM**: Dynamic statistical parametric mapping
**ECG**: Electrocardiogram
**EEG**: Electroencephalogram
**ESI**: EEG source imaging
**eLORETA**: Exact low-resolution electromagnetic tomography analysis
**EOG**: Electrooculography
**EPI**: Echo planar imaging
**FDM**: Finite difference method
**FEM**: Finite element method
**FLAIR**: Fluid-attenuated inversion recovery
**fMRI**: Functional magnetic resonance imaging
**GANTT**: Generalized activity normalization time table
**GDPR**: General data protection regulation
**GUI**: Graphical user interface
**ICA**: Independent component analysis
**IDIBAPS**: Institut d'Investigacions Biomèdiques August Pi I Sunyer
**IFCN**: International Federation of Clinical Neurophysiology
**ITI**: Inter-trial interval
**LORETA**: Low-resolution electromagnetic tomography analysis
**MEG**: Magnetoencephalography
**MNE**: Minimum Norm Estimation
**MRI**: Magnetic resonance imaging
**OS**: Operating system
**PCs**: Principal component(s)
**PCA**: Principal component analysis
**sLORETA**: Standardized low-resolution electromagnetic tomography analysis
**SPECT**: Single-photon emission computerized tomography
**SWOT**: Strengths weaknesses opportunities and threats
**WM**: White matter

# 1. INTRODUCTION

Over 80 years ago the electroencephalography (EEG) was first described with the promise of it providing a “window into the brain”. However, the transparency of this window has been obscured in the sense that sources in the brain that produced the signals on the scalp were not readily visible. [1] The recorded electrical signals generated by the brain are conducted through the cerebrospinal fluid, skull, and scalp. This process of volume conduction effectively blurs the EEG signals measured on the scalp, limiting the spatial resolution of these signals. [2]

The activity recorded at any head surface sensor reflects a summation of all active sources in the brain, superposed as a function of their distance, orientation, and resistivity of underlying tissues. Therefore, realistic source analysis of EEG potentials requires objective biophysical models that incorporate the exact positions of the sensors as well as the properties of head and brain anatomy, such that appropriate inverse techniques can be applied to map surface potentials to cortical sources.[3]

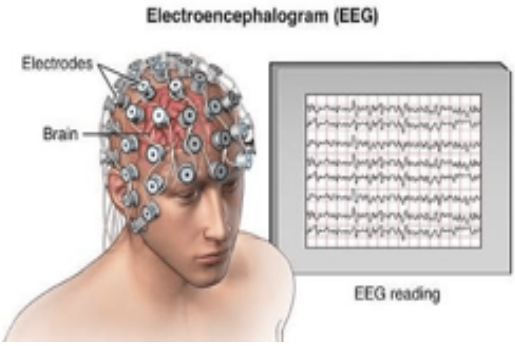


**Figure 1**: EEG recording [47]

The past decade witnessed an explosive development of functional neurological imaging techniques to observe and measure brain activity in humans. A variety of techniques for non-invasive measurements of brain activity have been developed, one of which is source localization using EEG. This technique uses the measurements of the voltage potential at various locations on the scalp (order of microvolts) and then applies signal processing techniques to estimate the current sources inside the brain that best fit this data. [4] EEG has enabled the estimation in the neural sources from the scalp potentials recorded through high-density sensors by solving the so-called “inverse problem”. Tremendous efforts have been made to integrate information across multiple modalities during the same task in an attempt to establish an alternative high-resolution spatiotemporal imaging technique [5].

The source reconstruction process can be divided into two main phases. First, it is needed to find the scalp potentials that would result from hypothetical dipoles (forward problem). Then, in conjunction with the actual EEG data measured at specified positions, it can be used to work back and estimate the sources that fit these measurements (inverse problem). The accuracy with which a source can be located is affected by a number of factors including head-modelling errors, source-modelling errors and EEG noise. [4]

In clinical applications, non-invasive localization of the active sources in the brain can be used to diagnose pathological, physiological, mental, and functional abnormalities related to the brain. Imaging modalities have been used to develop a better understanding of the functionality of the brain. Nevertheless, despite the good spatial resolution provided by imaging techniques such as MRI or CT among others, they fail on providing good time resolution. [1]On the other hand, EEG consists in a non-invasive electrophysiological technique of relatively high time resolution which is used to measure electric potential of brain neural activity. Taking, this into account, it can be said that a system capable of providing the time resolution of EEG and the spatial resolution of MRI would be very useful for determining regions of interest in the brain when dealing with neurological pathologies.

The kind of correlation between EEG and MRI and other imaging techniques will enable better understanding of many neurological disease, such as epilepsy, schizophrenia, Alzheimer's Disease and Anti-NMDAR Encephalitis, among many others. The advances in the diagnosis and treatment of brain abnormalities are highly dependent on the spatial and temporal resolution obtained throughout the acquisition techniques. EEG source reconstruction methods provide a good approach for achieving a mix of the advantages provided by the different techniques.

### 1.1. Objectives

IDIBAPS is an institute of basic translational and clinical research, there are several areas of investigation in which one can find groups focused on clinical and experimental neurosciences. This project aimed in providing a concrete technique for one of the groups in the neuroscience department, the group is leaded by Albert Compte and the department is focused in the area of theoretical neurobiology of cortical circuits. One of the lines of investigation of this group is "The NMDAR hypothesis of schizophrenia". This hypothesis is tested by comparing behavioral, EEG and fMRI parameters between encephalitic patients and patients with schizophrenia with control groups. The group needed to implement an analytical algorithm capable of localizing anatomical parts of the brain by using electrical activity (EEG) recorded during memory tasks. So far, the group had demonstrated that there is a difference in the electrical activity between patients and controls, but their methods could not determine where. The difference appeared to be in the alpha frequency of the EEG and was observed seconds before the experimental trials started. This difference allowed to differentiate between patients and control groups.

The motivation of this project arises from the need of Albert Compte's department to create a computing tool capable of localizing certain brain regions throughout the electrical information provided by the EEG of the patients and controls groups. The main goal of this project consisted in creating an appropriate source reconstruction algorithm by using a designed software toolbox specific for exploring, visualizing and analyzing human neurophysiological data. This algorithm had to be as generic as possible in order to be applied to the different groups.

Secondly, this source reconstruction algorithm had to be tested in all the participants of the investigation in order to obtain the activated sources during the trial. More specifically, since the findings of the IDIBAPS group revealed that the difference between the groups took place seconds before the trial started, the activated regions we were interested in finding were those which were active in that specific moment. These results enabled us to characterize which anatomical regions where producing the electrical differences among the groups.

### 1.2. Methods and structure of the project

In order to develop the localization system, a specific toolbox specialized in the analysis of neurobiological data was used. This software was MNE-Python [6] and covers multiple methods of data preprocessing, source localization, statistical analysis, and estimation of functional connectivity between distributed brain regions. This project was performed under the supervision of Albert Compte and was divided into six major phases.

First of all, it was essential to understand the basis of the inverse problem, and the software/packages/toolboxes capable of computing this technique. It was also necessary to determine which processing steps were needed to be implemented in order to compute the source reconstruction algorithm. To do so, comparisons with recent literature and a search of tutorials on these methods and how to apply them was an important step of the project.

The second phase consisted in the installation and familiarization of the software and packages that needed to be used: FreeSurfer [7] and MNE-Python [6,8] . During this phase, it was greatly important to start working with the different tutorials and examples provided by the chosen computational tools. These tutorials and examples were very useful for describing a correct pipeline. This phase ends with a description of the pipeline in which all steps required are described in detail.

The third phase started once the pipeline was defined. This phase consisted in testing, modifying, and applying the code by using one control subject. This phase needed to prove that the code is capable of solving the inverse problem.

The fourth phase consisted in confirming the biological sense of the results obtained by Albert Compte and his group. The validation was performed by analyzing the results obtained in a patient that represented an average of the information obtained from the data of control groups.

It is worth mentioning that the IDIBAPS group did not know which exact regions of the brain were being activated at a specific time of the recording of the EEG, but they have a deep understanding

on the trials performed by the patients. Therefore, they knew which regions had to be activated at some concrete times. These regions of activation allowed to validate the performance of the algorithm obtained.

The fifth phase started once the model was validated. The algorithm had to be used to evaluate the results for concrete set of EGGs recordings at a precise moment. The algorithm had to be run through every patient of the control group and encephalitic group. Afterwards, statistical analysis and machine learning algorithms were applied to the obtained data to conclude if there were patterns among the different patients.

The last phase consisted in an editing stage for writing the present report. First, a literature review was performed to understand the methods needed to compute the inverse problem by using MNE-Python package. In the detailed engineering section, it is described all the work done during the second to the fifth phases. Then, the technical and economical feasibility, timeline and legal aspects were studied. Last, the report ends with the conclusions extracted from the project exposed and a section in which future lines of research are discussed. This distribution follows the guide from the course 'Proyectos de Ingeniería' of the Biomedical Engineering degree at the University of Barcelona [9]. Therefore, in order to develop the different sections, all the indications and recommendations from the guide and the theoretical lessons of the course were taken into account. Finally, a presentation summarizing the information of the report will be presented in front of a jury on June 21st 2021.

### 1.3. Scope

Certain limitations were faced during the execution of this project. The main restriction of this project was the date of delivery of the project (June 2021). Another important limitation was the fact that as many other data analysis projects, specifically in the medical field, this project lacks from amount of data. This deficiency is a great limitation of many projects which try to establish a generalized criterion from the results obtained. On the other hand, the schizophrenic group of patients is not analyzed in this project since there were not enough EEGs recordings. Therefore, this project is focused on the study of the control group and the encephalitic group of patients. However, the algorithm is generic enough to be applied to the schizophrenic patients once all the needed data is obtained.

Considering the limitations mentioned above, the scope of this project included:

- Literature review on inverse problem and software/packages/toolboxes capable of solving the inverse problem.
- Analysis of the different examples and tutorials in order to create a personalized pipeline.

- Evaluate the algorithm obtained for an average of control patients and validate the results throughout specialist's opinions.
- Discussion of the results and errors detected.
- Apply the final algorithm at a concrete time, to different EEG sessions of the control groups and encephalitic groups and determine which are the active sources.

### 1.4 Location of the project

The present study has been conducted in collaboration with the Theoretical Neurobiological Cortical Circuits department at IDIBAPS research center. All the work has been performed at distance; however, the meetings were carried out with Albert Compte's group at the IDIBAPS center.

# 2. BACKGROUND

## 2.1. State-of-the-art

In order to have a better understanding of the field that this project covers, some concepts are defined and the state-of-art behind these concepts is presented. EEG and MRI are presented since they are two essential acquisition techniques needed during the estimation of active brain sources.

Also, it is important to get an insight in the state-of-the-art of the techniques used to find approximate solutions of the brain sources giving rise to the scalp potentials. However, the reader must keep in mind that the mathematical and physical principles behind these methods are beyond the scope of this project.

### 2.1.1. EEG

The electrical activity measured by scalp EEG recordings is generated by similarly oriented groups of cerebral cortical neurons near the scalp where the recording electrodes are placed. The majority of the electrical activity collected in the EEG is generated by groups of pyramidal neurons. The electrical activity recorded on the scalp represents the summation of the inhibitory or excitatory postsynaptic potentials from thousands of pyramidal cells near each recording electrode. This summated activity can be represented as a field with positive and negative poles (dipole). [10]

The distributed synaptic currents generate electromagnetic field, propagating within a passive volume conductor that comprises brain structure, cerebrospinal fluid, skull and scalp. The electrodes used, only detect activities of a large number of neurons which are synchronously electrically active. In a typical human adult EEG signal has a voltage range between 10 microvolts to 100 microvolts amplitude when measured in the scalp. [10]

Additionally, EEG waveforms are classified into five different frequency bands [10,11]:

- Delta (0.5-4 Hz): Slowest EEG waves, which are normally detected during the deep and unconscious sleep.
- Theta (4-8 Hz): They are observed during states of quiet focus.
- Alpha (8-14 Hz): They are the most dominant rhythms in normal subjects.
- Beta (14-30 Hz): Characteristic for the states of alertness, anxious thinking and focused attention.
- Gamma (over 30 Hz): Observed during active information processing.

The main advantages of an EEG system are its low costs, relative ease of use and excellent time resolution. For these reasons, EEG is widely used in many areas of clinical work and research.

However, an unfortunate reality of EEG is that cerebral activity may be overwhelmed by other electrical activity generated by the body or in the environment. Biological generated electrical activity (by scalp muscles, the eyes, the tongue, and even the distant heart) creates a massive voltage potential that frequently overwhelm and obscure the cerebral activity. [10] The approximate cost of a low-cost EEG system can range from values of 800-1,000€. However, there are more sophisticated systems which can achieve costs higher than 100,000€. For instance, the BioSemi Active two system has a 256-channel model which costs over 180,000€. [12]

A couple of examples of a state-of-the-art EEG systems are *TruScan* systems provided by *Deymed DIAGNOSTIC* [48], and the *Enobio EEG* systems by *Neuroelectrics* [49].

*Deymed-TruScan*:
*TruScan* is a family of EEG systems which offer state-of-the-art functionality for clinical EEG systems. The goal of *Deymed* consists in advancing the Neurology and Neurophysiology fields to new height with engineering innovation. Some of the advantages that a *TruScan EEG* has are the battery operated (lasting months on a single charge), the optical isolation (improving signal quality and patient safety) and wireless use, among others. The *TruScan EEG* system has a number of electrodes can range from 24 to 256. [48]

*Enobio EEG - Neuroelectrics*:
*Enobio* systems consist in a wireless medical grade EEGs for high precision EEG monitoring. These systems offer an integration with state-of-the-art tools for Brain Computer Interfacing (BCI) and Neurofeedback. Also, it is possible to perform a mobile brain imaging recording, so the exams can take place outside the lab for sports performance and consumer neuroscience research. The different *Enobio EEG* systems *Neuroelectrics* offers has a number of electrodes which ranges between 32 to 8 electrodes. The *Enobio 8* (8 electrode configuration) is one of the most precises systems in its class, this low number of electrodes has the advantages that the system becomes mobile, more comfortable and is ideal for out-of-the-lab and BCI applications. [49]

**Figure 2**: Enobio 8 by Neuroelectrics [49]

- **Electrode Montage**

EEG has been traditionally measured using the standard 10-20 electrode system. It has been widely acknowledged that the spatial resolution of the 10-20 system is not sufficient for modern brain research.[13] The first step in improving the spatial resolution of EEG is to increase the number of EEG electrodes which the market has respond to with commercially available systems including up to 256 electrodes. [10,14]

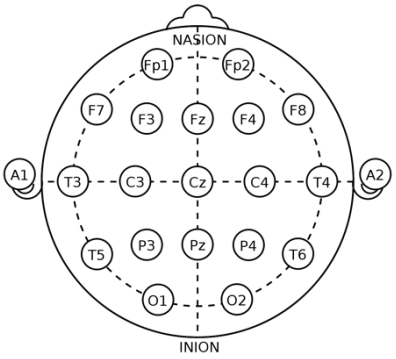


**Figure 3**: Electrode Montage [50]

A montage is a standardized arrangement and selection of channel pairs and chains for display and review. There are many different montages used for various purposes, but they are divided into two types: bipolar and referential. In a bipolar montage, neighboring electrodes are paired to one another, either anterior to posterior or side to side. Alternatively, referential montages link each exploring active electrode to a distant reference. [10,14]

According to the guideline of the International Federation of Clinical Neurophysiology (IFCN) the scalp electrodes should be placed at standard positions. The standard IFCN array is the extension of the so-called "international 10-20 system". [14] It uses stable anatomical points of the skull such as naison (point between the forehead and nose) and pre-auricular points (left and right). In this montage, the electrodes are spaced at 10% or 20% of the total distances between them. The standardized names of the electrode positions consist of two symbols. The first symbol is a letter abbreviation of the underlying brain region and the second is a number indication its more precise position within that region.[15]

- **Electrode digitazion**

In many studies, the electrode location has to be "digitized"; recorded digitally via a three-dimensional position recording method. These digitized locations can then be coupled with a subject-specific MRI or other imaging techniques.

Digitizing electrode locations is an essential step for setting up the head model. The digitizing process involves recording 3-D positions of the electrodes in a global coordinate system and transforming the locations from the global to the head coordinate system. This transformation requires that the two coordinate systems share anatomical landmarks (typically left per auricular, right per auricular, and nasion). [2,6]

### 2.1.2 Anatomical modelling

A Magnetic Resonance Imaging (MRI) is a sophisticated, non-invasive imaging technique used in hospitals and clinics to produce detailed soft tissue anatomical images. An MRI scan must be

obtained from each individual for doing subject-specific anatomical modelling. The anatomical information of the subject allows us to compute the forward operator which is the previous step that would lead us to the computation of the inverse modelling and the further obtention of the active sources. The accuracy of EEG source estimation depends crucially on the head model and the solution space initiated to compute the forward problem. 3 Tesla MRI is fundamentally applied in research and it costs from 1.9€-2.5€ million. [16]

It is worth mentioning that a CT scan could also be used to create the anatomical model of a subject, however, there is no sufficient indication to expose a subject/patient to the harmful ionizing radiation produced during CT scan. [13]

The information provided by an MRI scan allows us to compute essential components involved in source reconstruction. These are the source-space and the head model. The source space represents a set of coordinates where the candidate's dipoles are allowed to have nonzero amplitudes. The sources are constrained to reside only in the gray matter volume; however, this volume is modeled as a surface since the available technology does not have the spatial resolution to discriminate sources at different cortical layers. [17,18]

On the other hand, the head models are created to capture the geometries and conductivities of head tissues (the scalp bone, cerebral spinal fluid, white matter, gray matter, eye compartments, and eyeballs). There are two main types of volume conductors (head models): the simple models and the realistic head models. The former is based on a single layer sphere, or even a 3-4-layer spheres. [17] These simple models are much simpler and faster when compared to the realistic models, however these models lack on accuracy. The realistic head models are numerical solvers which despite being computationally complex, they represent more accurately the head shape.

There are three different realistic models:

- Finite Difference Model (FDM)
- Boundary Element Model (BEM)
- Finite Element Model (FEM)

In this project, BEM model was considered since its computational performance and demands surpassed the other two methods. The BEM surfaces are the triangulations of the interfaces between different tissues needed for forward computation. These surfaces are the inner skull surface, the outer skull surface and the scalp surface. The volume conductor properties in this model are approximated to be realistically shaped compartments of isotropic and homogenous conductivities. [19]

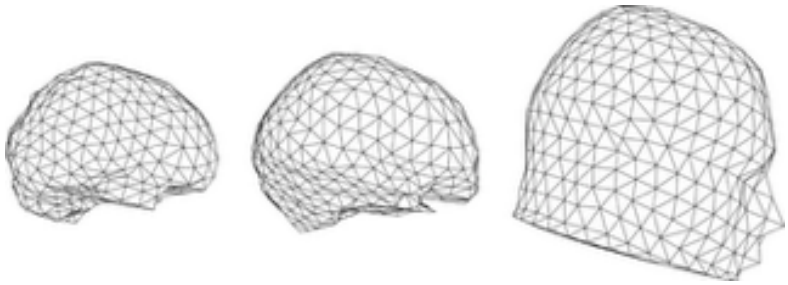

**Figure 4**: Example mesh of the human head used in BEM; triangulated surfaces of the brain, skull and scalp compartments [20]

### 2.1.3. Inverse Problem

The source reconstruction process can be divided into two main phases. First, it is needed to find the scalp potentials that would result from hypothetical dipoles (forward problem). Then, in conjunction with the actual EEG data measured at specified positions, it can be used to work back and estimate the sources that fit these measurements (inverse problem). The accuracy with which a source can be located is affected by a number of factors including head-modelling errors, source-modelling errors and EEG noise. [4]

Localization based on EEG depends directly on the ability to make a reasonable guess about current sources and their locations based on measurements from the surface. Unfortunately, theory shows that there is not a unique solution to this problem. The inverse problem is an ill-posed problem prone to ambiguities. [21]

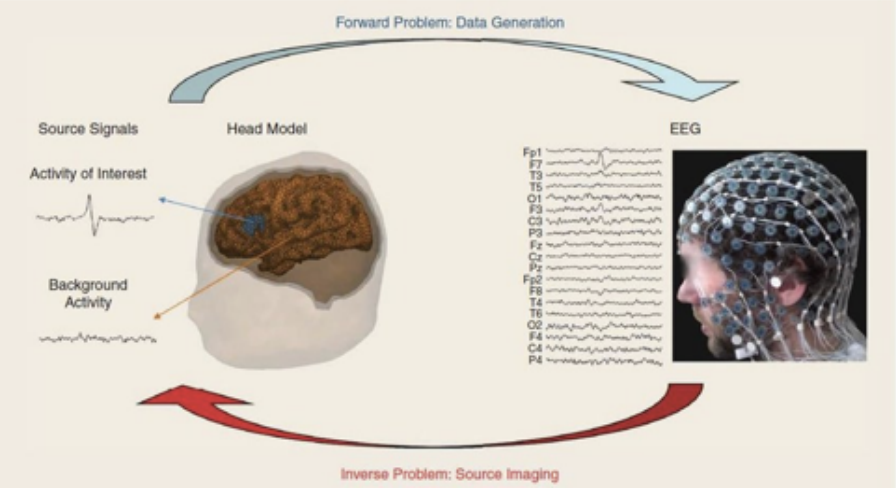


**Figure 5**: An illustration of the forward and inverse problems in the context of EEG [22]

The ill-posed nature of this problem arises from the fact that two different sources might produce the same measurement. [13] Actually, since the number of electrodes is lower than the number of possible sources, we face a problem in which there is further less data observed than data to recover. [23]

The EEG inverse problem is an ill-posed problem because for all admissible output voltages, the solution is not unique and unstable (the solution is highly sensitive to small changes in the noisy data). There are various methods to remedy the situation, they imply establishing certain constraints regarding the dipoles magnitude(s), position(s), and orientation(s).[4][24]

There are two main approaches to the inverse solution: non-parametric methods and parametric methods. These methods are analysed in the next section; however, it is worth mentioning that this project is focused on non-parametric methods since the MNE-Python toolbox provides excellent workflows, examples, and tutorials on these methods. [6,8,25]

### 2.1.4. Inverse solutions

There are various methods which can be applied in order to solve the inverse problem. Regarding the EEG inverse problem, there are six parameters that specify a dipole: three spatial coordinates (x, y, z) and three dipole moment components (orientation angles and strength), these may be reduced if some constraints are places on the source. [4]

As mentioned before, there are two main approaches to the inverse solution, non-parametric and parametric. In non-parametric approaches several dipoles sources with fixed locations and possibly fixed orientations are distributed in the whole brain volume or cortical surface. Due to the orientation of the pyramidal neurons, the orientation of the dipoles is set to be normally aligned. The amplitudes of these dipoles are then estimated. Since the dipole location is not estimated, the problem becomes a linear one. Several algorithms have been developed with a minimum of localization error and high resolution and less computational time. Some examples of non-parametric algorithms are minimum norm estimation (MNE), low-resolution electromagnetic tomography (LORETA), and dynamical statistical parametric mapping (dSPM). [21]

The MNE solution provides great results in terms of resolution and current estimation, however, it fails to address the issue of deep source localization. On the other hand, LORETA provides smoother and better localization for deep sources with fewer localization errors. Disadvantages of this technique are low spatial resolution and blurred localized images of a point source with dispersion in the image. dSPM can also be considered as an alternative approach to compensate for depth bias. [4]

During recent years, several practical methods have been proposed to localize the sources of brain activities using EEG signals. However, there is a requirement for greater understanding of computerized EEG source localization techniques to optimize treatment and patient care in brain functional disorders. It is important to remark the fact that the accuracy with which a source can be

located is affected by a number of factors including head-modelling error, source-modelling errors and EEG noise (instrumental or biological).[20]

### 2.3. State of the situation

MNE-Python is an open-source software package that addresses the challenge of characterizing and locating neural activation by providing state-of-the-art algorithms implanted in Python. These algorithms cover multiple methods of data processing, source localization, statistical analysis, and estimation of functional connectivity between distributed brain regions. MNE-Python has some dependencies on the FreeSurfer software for the computation of the head model. [6]

Although MNE-Python is a good option when working with EEG data, there exist several powerful commercial or academic packages for EEG source imaging which should be mentioned. There are multiple academic software packages for EEG data processing, e.g., Brainstrom, EEGLAB, Field-Trip, NutMeg and SPM, all implemented in Matlab, with some dependencies on external packages such as OpenMEEG for BEM forward modelling or NeuroFEM for FEM forward modelling. Also, widely used commercially available software packages for EEG source localization are BESA, Curry, GeoSource, and BrainVision Analyzer. [6,8]

The following table illustrates some of the available software and their websites in which someone can use in order to solve the inverse problem when considering EEG signals. Each software packages present certain algorithms capable of performing source reconstruction on EEG. All the data has been acquired from [21].

| Name | Website | Inverse Methods |
|---|---|---|
| **Academic Packages** | | |
| Brainstorm | https://neuroimage.usc.edu/brainstorm/ | Dipole modeling, Beamformer, sLORETA, dSPM |
| Cartool | https://sites.google.com/site/cartoolcommunity/ | Minimum Norm, LORETA, LAURA, Epifocus |
| EEGLab | https://sccn.ucsd.edu/eeglab/download.php | Dipole modeling |
| FieldTrip | http://www.fieldtriptoolbox.org/ | Dipole modeling, Beamformer, Minimum Norm |
| LORETA | https://www.uzh.ch/keyinst/loreta.htm | LORETA, sLORETA, eLORETA |
| MNE | https://mne.tools/stable/index.html | MNE, dSPM, sLORETA, eLORETA |
| NUTMEG | https://www.nitrc.org/projects/nutmeg/ | Beamformer |

| | | |
|---|---|---|
| SPM | https://www.fil.ion.ucl.ac.uk/spm/ | dSPM |
| **Commercial Packages** | | |
| BESA | https://www.besa.de/products/besa-research/besa-research-overview/ | Dipole modeling, RAP-MUSIC, LORETA, sLORETA, LAURA, SSOFO |
| BrainVision Analyzer | https://www.brainproducts.com/ | LORETA |
| BrainVoyager | https://www.brainvoyager.com/ | Beamformer, Minimum Norm, LAURA, LORETA |
| GeoSource | https://www.usa.philips.com/healthcare/product/HC6150036/geosource-2-clinical-esi-software | Minimum Norm, LAURA, LORETA, sLORETA |
| CURRY | https://compumedicsneuroscan.com/curry-7-signalprocessing-basic-advanced-source-analysis/ | Minimum norm, sLORETA, eLORETA, SWARM |

Table 1: Software packages available online to solve the inverse problem

The decision regarding which software should be used when analysing EEG signals for source localization comes with many constraints, for instance the amount of money the programmer is willing to spend. Also, it should be taken into account the preferences and expertise the programmer has regarding the programming environment. Another important fact consists in evaluating which are the options that each software/package allows its users to work with. It is greatly important to know the different tools and dependencies each software package will need; this should be taken into account in order to find the package that best fulfils the expectations of the programmer.

# 3. MARKET ANALYSIS

## 3.1. Sectors to which it is directed

During recent decades, brain source modelling by EEG has been an active area of research. In clinical applications, non-invasive localization of the active sources in the brain can be used to diagnose pathological, physiological, mental, and functional abnormalities related to the brain.

It is shown that different brain source localization techniques are effective in the diagnosis and treatment of several brain abnormalities and diseases. Among the brain abnormalities that have been investigated using EEG source localization methods, epilepsy and attention-deficit hyperactivity disorder (ADHD) have more contribution. [1]

Electric brain imaging has been used extensively in the area of neurophysiological and psychology-related research for the past two decades. Investigating non-invasive source localization approaches can help accelerate the diagnosis and treatment of functional diseases of the brain.[26]

## 3.2. Historical evolution of the market and future market prospects

The investigation in [22] demonstrated how the number of studies conducted in the lines of investigation of source reconstruction is increasing as times goes by. The researchers selected 120 studies which tackled the inverse problem in different ways. It was seen that only 10% included in the 120 studies were published in between 1980 to 2000. On the other hand, 32.5% of the reviews found were published by the end of 2010. Finally, 57.5% were published in between 2011 and 2018. These kinds of studies mainly come from biomedical research institutes which try to improve the diagnosis, treatment and tracing of neurological diseases.

The role of source localization algorithms has been accelerated mainly in the areas of diagnosis and treatment of various diseases. On the other hand, the effect of psychiatric drugs on the activity of the brain sources has been less considered. Nevertheless, it is very probable that in the future we will have more information on these fields. [22]

Some relatively new applications of the EEG source localization technique are:

- Brain-Computer Interfaces:

Brain-Computer Interface (BCI) is an effective as well as powerful tool for user-system communication. BCI can be described as a machine learning system, which recognizes a certain set of patterns in control signal acquired directly from user's brain. [11,27] Every BCI system has essentially five components: brain activity measurement, pre-processing, feature extraction, classification, and translation into a command. The measurements of the brain activity are usually

extracted throughout an EEG system and source localization methods can be used to localize active areas of the user's brain, and hence, represent the EEG signal by its spatial features. [11] The outcomes of the classification phase are translated into device commands to develop real-life applications.

There are a considerable number of popular BCI applications, such as wheelchair control, BCI mobile robot (like a robotic arm), BCI cursor control, BCI spellers, emotion recognition using EEG, biometrics, and virtual reality and gaming. Although conventional BCI systems have made tremendous advances in the past few decades, nonetheless, the research still faces significant challenges in EEG classification. The challenges include various biological and environmental artifacts in EEG, a low SNR, and dependency on human expertise for extracting meaningful features.[11]

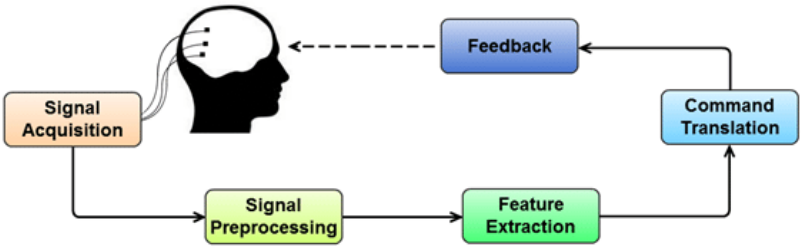


**Figure 6**: Functional architecture of a typical BCI [11]

- Epilepsy:

EEG source imaging (ESI) has proven to be an important tool to localize the epileptogenic focus and to decide about the possibility for surgical resection or guide the placement of intracranial electrodes. Contrary to presurgical diagnostic methods like MEG, fMRI, and SPECT, EEG data are already available for almost every patient undergoing presurgical evaluation worldwide. The ESI achieves similar sensitivities and specificities as SPECT and MEG, but tracers or additional scanning facilities are not required, and it is highly cost-effective. [28]

In theory, the ESI could be easily included in the phase of evaluation process. In addition, in certain situations, patients may benefit from less diagnostic procedures, financial costs could decrease, and patient throughput can be increased. Nevertheless, and despite many promising results, the method has not yet found its way into clinical practice. At present, ESI seems to be a promising technique that can positively contribute to visual EEG analysis in localization of epileptic spikes. [29]

- Hyperscanning:

Hyperscanning techniques offer a new approach to account for the complexity in the examination of social interactions as a whole. The idea of hyperscanning consists in measuring the activity of multiple brains simultaneously. The methods considered in hyperscanning research are those that can measure the brain activity, such as EEG, MEG, and fMRI. [30]

The EEG-based hyperscanning technique provides an approach to explore dynamic brain activities between two or more interactive individuals and their underlying mechanisms. This technique has been applied to study different aspects of social interactions since 2010. [30,31] This is an emerging approach in computational psychiatry and the incorporation of ESI in these analyses might give interesting insights regarding the differences in the active sources during the social interaction of individuals.

### 3.3. Product environment

The evaluation of the inverse problem regarding the localization of brain sources has not only been studied by using the electrical information obtained in an EEG signal. There is a similar technique which has received a lot of attention in these lines of investigation.

Magnetoencephalography (MEG) represents a noninvasive functional brain imaging method, just like EEG, whose extracranial recordings measure extremely weak magnetic fields generated by the electric activity of the neural cells. [13,32] In the beginning of biomagnetic research there was a lot of hope that biomagnetic signals would include information independent on the bioelectric signals. [10] However, it has been demonstrated that MEG and EEG techniques in terms of source localization offer similar information about brain sources in what concerns accuracy, and spatiotemporal resolution. Regarding the cost of this technique, the MEG instrumentation costs about 20 times more than the EEG instrumentation with the same number of channels. [10]

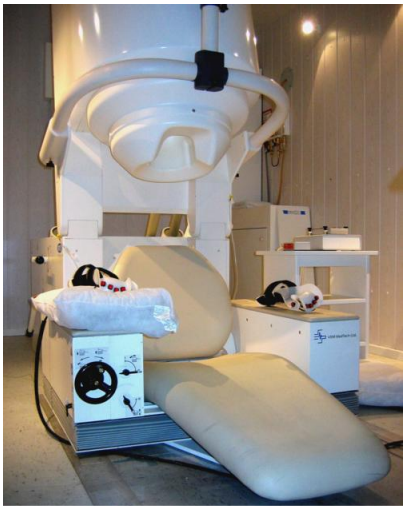

**Figure 7**: Example of a MEG equipment [51]

The current role of magnetic source localization, using MEG data, is not fully established yet, but is considered useful as an additional tool in the presurgical pathway. It has been recognized as a useful and accurate clinical tool in several centers of Europe, Japan, Korea and North America.[33]

# 4. CONCEPTION DESIGN

In this section, the considered programming environments, toolboxes, and software capable of performing source reconstruction on EEG are discussed. As it has been previously mentioned, there exist multiple packages, and software that could have been implemented for the execution of this project (Table 1). The different studied options are shown in Table 2.

| | **Studied Solutions** |
|---|---|
| **Programming environment** | - Matlab<br>- Python |
| **Packages** | - MNE-Python<br>- FieldTrip<br>- Brainstorm |
| **Anatomical reconstruction software dependencies** | - FreeSurfer<br>- Open MEEG BEM |

**Table 2**: Studied solutions

## 4.1. Solutions study

Commercial software packages might represent the best choice with respect to support, documentation, and performance. However, these software were not considered as possible programming environments. Academic software packages are evolving constantly to address new imaging challenges, and they offer a flexibility and a reactivity that commercial software do not offer.[34] Also, and not less important, the fact that academic software are free was a compelling reason for the final decision. On the other hand, the proposed packages were reduced down to the top three leading software in the M/EEG data analysis. [35]

### 4.1.1. Solution 1: MNE-Python

MNE is an academic software package that aims to provide data analysis pipelines encompassing all phases of M/EEG data processing. This software consists of three core subpackages which are fully integrated: the original MNE-C, MNE-Matlab, and MNE-Pyhton. [6,8]

The MNE-Python code is the most recent addition to the MNE software; it started as a reimplementation of the MNE-Matlab code, removing any dependencies on commercial software. MNE-Python provides several additional features, such as time-frequency analysis, non-parametric statistics, and connectivity estimation. [6,8]

The MNE software, in particular the MNE-Python project, is developed and maintained to work toward high quality in terms of accuracy, efficiency and readability of the code. Neuroimaging is a

broad field encompassing static images, such as anatomical MRI as well as dynamic, functional data such M/EEG or fMRI. The MNE software relies on other packages such as FreeSurfer for anatomical MRI processing, or Nibabel for reading and writing images such as standard NIfTI files. In addition, MNE-Python is tightly integrated with the core python libraries for scientific computation (NumPy, SciPy) and visualization (matplotlib and Mayavi). [6,8]

An extensive set of example scripts exposing typical workflows or elements thereof while serving as copy and paste templates are available on the MNE website and are included in the MNE-Python code. The MNE software also provides a sample dataset consisting of recording from one subject combined M/EEG conducted at the Martinos Center of Massachusetts General Hospital. This dataset can serve as a standard validation dataset for M/EEG methods, hence favouring reproducibility of results. [6,8]

MNE offers a tight integration with the anatomical reconstruction provided by the FreeSurfer software, as well as a selection of inverse solvers for source imaging. Different available algorithms for solving the inverse problem are MNE, dSPM, sLORETA, and eLORETA. [6,8,34]

Although MNE-Python has only been under heavy development for a couple of years, it has rapidly evolved with expanded analysis capabilities and pedagogical tutorials because multiple labs have collaborated during code development to help share best practices. [6]

#### 4.1.2. Solution 2: FieldTrip

Another option considered as a possible programming package was FieldTrip. FieldTrip is a Matlab-toolbox for the analysis of MEG, EEG, and other electrophysiological data. It offers pre-processing and advanced analysis methods, such as time-frequency analysis, source reconstruction using dipoles, distributed source and beamformers and non-parametric statistical testing. It supports the data formats of all major MEG systems and the most popular EEG systems. The FieldTrip toolbox allows experimental scientists to have access to state-of-the-art data analysis algorithms. The FieldTrip wiki contains a large amount of documentation for facilitating the use of the toolbox, including tutorial documentation, answers to frequently asked questions and example Matlab code. [36]

Different source reconstruction algorithms are available for the estimation of the location and strength of neuronal activity, including dipole fitting based on nonlinear optimization, scanning methods such as minimum variance beamformers in the time and frequency domain, and linear estimation of distributed source models. [21,36]

The open-source development model of FieldTrip has proven to be very effective, on the one hand creating a large well-tested collection of Matlab functions, on the other hand resulting in a large contribution to experimental neuroscience. [34,36]

There exist many courses and workshops of the past years with a lot of information about neuroimaging analysis. The tutorials allow the user to get started by working with copy-and-paste examples.

### 4.1.3. Solution 3: Brainstorm

Brainstorm is a collaborative open-source application dedicated to MEG and EEG data visualization and processing, with an emphasis on cortical source estimation techniques and their integration with MRI data. The primary objective of the software is to connect MEG/EEG neuroscience investigators with both the best-established and cutting-edge methods through a simple and intuitive graphical user interface (GUI).[34,35]

Brainstorm software is written almost entirely in Matlab scripts. One important feature for users who do not own a Matlab license is that a stand-alone version of Brainstorm, generated with the Matlab Compiler, is also available for download for Windows and Linux operating systems.

All software functions are accessible through the Graphical User Interface (GUI), without any direct interaction with the Matlab environment; hence, brainstorm can be used without programming experience. [35]

### 4.1.4. Summary of possible solutions

| Featured software packages | MNE | FieldTrip | BrainsStorm |
|---|---|---|---|
| Time-series analysis | | | |
| Time-frequency analysis | | | |
| Forward modelling | | | |
| Source modelling | | | |
| Functional or effective connectivity | | | |
| Statistical analysis | | | |
| Graphical User Interface | | | |
| Interoperability (other software/packages) | Matlab | BESA, EEGLAB, LORETA, SPM8 | User plugins |
| Environment/OS | C/C++, Matlab and Python | Matlab | Matlab |

| | | | |
|---|---|---|---|
| Unique feature(s) | High-quality 3D graphics; computationally efficient | Community-based development; extensive documentation; real-time features | Emphasis on user interaction through GUI or scripts |

**Table 3**: Summary of software features [34]

### 4.2. Proposed solution

In light of the above, the chosen solution for this project was MNE-Python. Several considerations were taken into account during this decision. First, FieldTrip was rejected due to the fact that it needs a Matlab license in order to work with these packages. The objective of this project was not only to obtain source localization results, but also provide a useful pipeline for the clinicians in IDIBAPS. Since the code might be implemented again for further studies, they were not interested on the need of using commercial programming environments such as Matlab. On the other hand, although Brainstorm does not require a Matlab license, this application was rejected since it did not require any programming knowledge and did not offer the flexibility that Python environment offers.

# 5. DETAILED ENGINEERING

The IDIBAPS research group, headed by Albert Compte, is actively working in finding the differences between the electrical activity of an encephalitic group with respect to a control group. So far, they have demonstrated that these differences exist, and they have localized them in a concrete frequency band of the EEG signal, the alpha band. Also, these differences among the two groups were observed seconds before the trial started. A frequency analysis performed over the EEG signal demonstrated that these differences were located in the alpha band.

However, it was needed to localize which brain regions were leading to those differences. Therefore, the main objective of this project consisted in observing which regions where active instants before the trial started. The resulting information would be highly informative to the researches since it would allow them to improve the interpretation of their results from the anatomical point of view. Also, this project aimed in producing a detailed pipeline which could be followed by the researchers in case more data was obtained and the analysis had to be repeated.

The following sections introduce the initial data, a pipeline presenting the steps undertaken to solve the source localization problem, and a discussion of the final results obtained.

## 5.1. Initial data

This section introduces the initial data that was handed to the developer of this project in order to locate the sources from the EEG data of patients and control groups. It is described the experimental sample, the trial description, and the EEG and MRI data processing. All the information exposed in the following sub-sections was handed to the main developer of this project by Albert Compte.

### 5.1.1. Experimental sample

The sample included was n = 9 patients with anti-NMDAR encephalitis (enc; age 28.7 ± 11.3 years, mean ± s.d.), and n = 7 neurologically and psychiatrically healthy control participants (ctrl; age 24.9 ± 10.4 years, mean ± s.d.), all with normal or corrected vision. Patients with anti-NMDAR encephalitis were recruited from centers in Spain, Germany, and the United Kingdom and participated in the experiment several months after hospital discharge. Controls were recruited from the Barcelona area. All healthy controls tested seronegative for antibodies against NMDAR in serum.

### 5.1.2. Trial description – memory task

Participants completed one 1.5 h session performing a visuospatial working memory task. Each trial began with the presentation of a central black fixation square on a grey background (0.5 x 0.5 cm) for 1.1 s. A single coloured circle (stimulus, diameter 1.4 cm, 1 out of 6 randomly chosen colours with equal luminance) was then presented during 0.25 s at one of 360 randomly chosen angular locations at a fixed radius of 4.5 cm from the center. When the fixation dot changed to the stimulus' colour (probe), participants were asked to respond by making a mouse click at the remembered location (response). A white circle indicated the stimulus' radial distance, so participants only had to remember the angular position. After the response, the cursor had to be moved back to the fixation dot to start a new trial (ITI). Participants were instructed to maintain fixation during the fixation period, stimulus presentation, and memory delay and were free to move their eyes during response and when returning the cursor to the fixation dot.

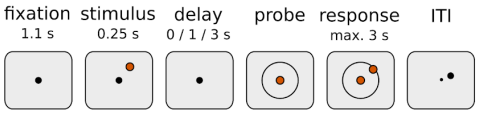


**Figure 8**: Trial illustration

At the end of each trial, the electrical activity recorded was stored in two files. The first is known as longepoch and the other as respepoch. Although both files have the exact same information, they are centered (t=0s) at different moments of the trial. In the longepoch, at time equal 0 seconds, the visual stimulus is presented. On the other hand, in the respepoch file the second 0 corresponds to the moment in which the patient is moving the mouse.

### 5.1.3. Processing EEG data

EEG was recorded from 43 electrodes attached directly to the scalp. The electrodes were located at Modified Combinatorial Nomenclature sites Fp1, Fpz, Fp2, AF7, AFz, AF8, F7, F3, Fz, F4, F8, FT7, FC3, FCz, FC4, FT8, A1, T7, C5, C3, Cz, C4, C6, T8, A2, TP7, CP3, CPz, CP4, TP8, P7, P3, Pz, P4, P8, PO7, PO3, POz, PO4, PO8, O1, Oz and O2. Sites were referenced to an average of mastoids A1 and A2 and re-referenced offline to an average of all electrodes. It was further recorded horizontal EOG from both eyes, vertical EOG from an electrode placed below the left eye and ECG to detect cardiac artifacts.

EEG data was pre-processed using Fieldtrip (version 20171231) in MATLAB R2017b and R2019a. Outlier trials were excluded in which variance or kurtosis across samples exceeded 4 standard deviations from mean variance or kurtosis over trials, respectively. To reduce artifacts in the remaining data, an independent component analysis (ICA) was ran on the trial-segmented data

and corrected the signal for blinks, eye movements, and ECG signals, as identified by visual inspection of all components.

All the data regarding the electrode's positions, electrodes labels and the position of anatomical landmarks were stored in a .txt file known as *neuronavigation* file. Each patient had their own file.

#### 5.1.4. Anatomical Sample

MR structural imaging was conducted in the Magnetic Resonance Image Core facility of IDIBAPS, on a research-dedicated 3 Tesla Prisma scanner (SIEMENS) using a 64-channel head coil, located in the Hospital Clinic. The full scanning session took 85 min, including 3D T1-weighted in sagittal plane; axial functional EPI during a human WM task; T2*-weighted axial EPI; axial diffusion weighted EPI; 3D sagittal FLAIR; and glutamate and H2O univoxel spectroscopy in dorsolateral prefrontal cortex and hippocampus. Only 3D structural images (T1) were used for this project.

### 5.2. Pipeline implemented

One of the most important aspects, when working with any package/toolbox implemented in any programming environment, consists in introducing the correct input parameters, and use a concrete format in order to obtain the desired outputs. When working with MNE this is not different. It is essential to introduce the precise and specific inputs the MNE functions need. The following pipeline describes all the steps and necessary inputs that need to be followed and introduced in order to compute source reconstruction of EEG data.

This pipeline introduces some of the MNE functions which need to be used and is based on the pipeline found in two different MNE tutorials. [6,8] Although the pipeline implemented came mainly from these two tutorials [52] and [53], many tutorials which should be mentioned have become particularly useful in some of the steps of this pipeline. [54-59] The code implemented to perform this pipeline can be found in the annexes. (12.5)

#### 5.2.1. Installation

To get started some installations need to be performed. First, Anaconda, the world's most popular Python distribution platform, was installed. It is strongly recommended by MNE to use Anaconda since it includes the *conda* command line tool for installing new packages and managing different package sets ("environments") for different projects. The installation process of Anaconda can be found in [37].

Secondly, MNE needs to be installed. To do so, one should follow the instructions found in [60]. Finally, in the MNE ecosystem, the FreeSurfer software is used to convert structural MRI scans

into models of the scalp, inner/outer skull, and cortical surfaces. Therefore, the FreeSurfer software has to be installed. All the system requirements, setup instructions, and test scripts are provided on [7].

### 5.2.2. Reconstruction anatomical MRI using FreeSurfer

After installation, the reconstruction of structural MRI has to be executed for each subject. This is an essential step since all the head model depends on the surfaces created during the reconstruction.

The commands needed to perform the reconstruction can be done in the terminal of one's computer. First, it is necessary to set up the FreeSurfer environment by creating the variables FREESURFER_HOME and SUBJECTS_DIR. The first corresponds to the location of the FreeSurfer software and the second variable corresponds to the location of the subject's directory in which the user will find the final results of the reconstruction process. Then, the function *recon-all* needs to be introduced in the terminal indicating the name of the subject (this will be the name of the final folder in which all reconstructions can be found). Another important input of this function is the location of the MRI scans. An example of how this code should be implanted can be found in the annexes (12.1).

### 5.2.3. Processing EEG data

EEG data analysis typically involves three types of data containers coded in MNE-Python as Raw, Epochs and Evoked objects. The raw data comes straight out of the acquisition system; these can be segmented into pieces often called epochs or trials, which generally correspond to segments of data after each repetition of a stimulus. These segments can be averaged to form evoked data (figure 10). On the other hand, the containers share some common attributes such as the channels name, and an info attribute which is a modified Python dictionary storing all the metadata about the recoding. The info attribute contains information such as the sampling frequency, the channels types and positions, the positions of the head digization points used for coregistration, and a list of bad channels. [6,8,25]

As explained before, the IDIBAPS research group had already processed the raw data and transformed it into the trials format. Therefore, the starting point regarding the initial structure of the EEG data was in the object known as epochs or trials. On the other hand, the info attribute was created using the neuronavigation files which contained all the information regarding the electrode's positions, labels, etc.

After importing the epochs and creating the info attribute, a noise covariance matrix needs to be calculated (figure 9). The MNE software employs an estimate of the noise-covariance matrix to weight the channels correctly in the calculations. The noise covariance matrix provides information about field and potential patterns representing uninteresting noise sources of either human or environmental origin. This is an important step since many methods in MNE, including source estimation, require noise covariance estimations from the recordings. Finally, the epochs have to be averaged to create evoked data which will be used to compute the inverse solution.

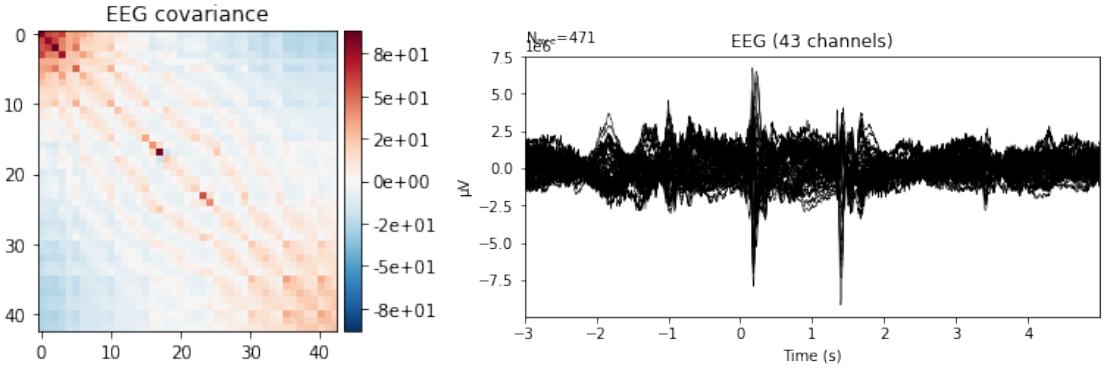


**Figure 9 and 10**: Noise covariance matrix and evoked data.

### 5.2.4. Forward operator

As mentioned before, the forward operator consists in finding the scalp potentials that would result from hypothetical dipoles. To solve the forward problem, one needs an approximation of the distribution of the electrical properties of the head, the specifications of the elementary source model and the source space, and the locations of the EEG locations on the scalp.

- Compute BEM surfaces and model

BEM surfaces are the triangulations of the interfaces between different tissues. These surfaces are the inner skull surface, the outer skull surface and the outer skin surface. In order to create the BEM model, it is needed first to segment the different surfaces by using FreeSurfer software, and then one can use MNE to create the head model which describes geometrical and conductivity properties of the subject's head.

MNE relies on FreeSurfer for the automatic segmentation of the skull and scalp surfaces. Therefore, computing the BEM surface in MNE requires FreeSurfer and makes use of the command-line tool mne watershed_bem(). The entire explanation about the command-lines needed to compute the BEM surfaces can be found in the annexes (12.2).

The creation of a BEM model describes the geometry of the head, and the conductivities of the different tissues. MNE supports three-compartment boundary element model and the default

electrical conductivities used are 0.3S/m for the brain and the scalp, and 0.006S/m for the skull. The conductivity of the skull is assumed to be 1/50 of that of the brain and the scalp. [26] This BEM model is independent of the EEG data and the head position. The command-line needed to compute the BEM model *is mne.make_bem_model()*, and the input attributes are the subjects directory in which the FreeSurfer reconstruction can be found, and the selected conductivities.

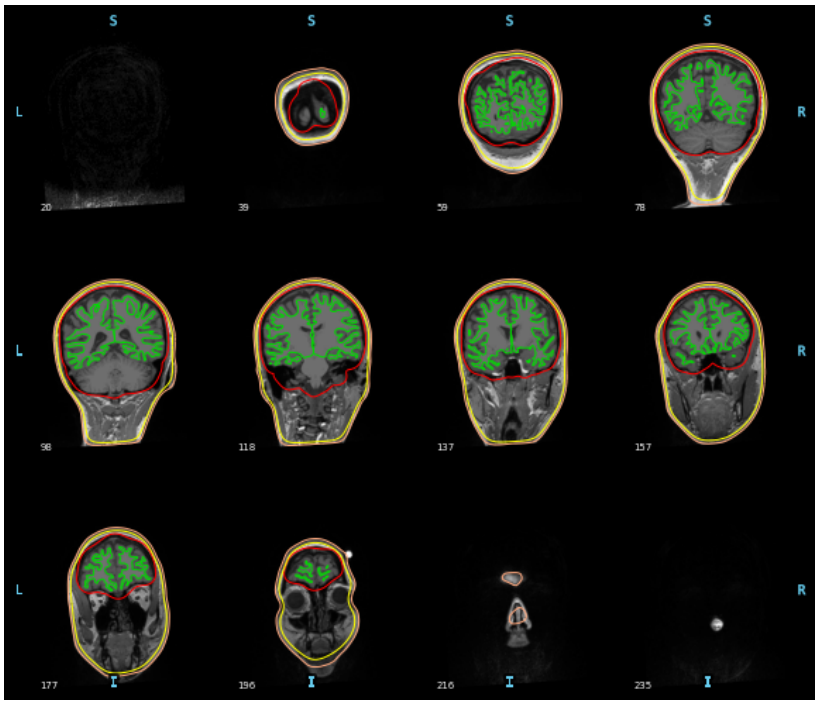


**Figure 11**: Surfaces segmented by FreeSurfer

- Co-registration

The forward solver requires that the boundary-element surfaces, the source space, and the sensor locations are defined in a common coordinate system. This is made possible by the co-registration step, which outputs the rigid-body transformation that relates the MRI coordinate system employed in FreeSurfer and the "head" coordinate system, designed by the anatomical landmarks.

In MNE software the transformation to align the head and the sensors is stored in a so-called trans file. It is a FIF file that ends with -trans.fif. It can be obtained with the convenient command line *mne coreg*(). Once this command line has been run, a GUI appears and the user needs to insert the digitazion montage from the info attribute, the anatomical landmarks of the patients during the EEG recording and indicate the folder where the MRI anatomical reconstruction can be found. If all this information is introduced, the GUI allows the user to save the trans file.

- Source Space

The locations of the elementary dipolar sources need to be specified a priori to compute the forward operator. Setting up the source space is a stage which consists in creating a suitable decimated dipole grid on the white matter surface. To create the source space, MNE uses a repeatedly

subdivided icosahedron or octahedron as the subsampling method. For real analysis, the recommended spacing is an octahedron with 6 subdivisions.

There are two types of source spaces:

- Surface-based source space when the candidate's sources are confined to the cortical surface
- Volumetric or discrete source space when the candidate's sources are discrete, arbitrarily located points inside the brain and bounded by the surface.

In the case of the surface-based type, the source space contains two parts, one for the left hemisphere and one for the right hemisphere.

In this project surface-based source space has been used to compute the forward operator. The command-line needed to compute the source space is *mne.set_up_source_space(),* and the inputs of this function is the directory in which one can find the MRI anatomical reconstructions executed by FreeSurfer, and chosen subsampling method, due to MNE recommendations, octahedron with 6 subdivisions is used.

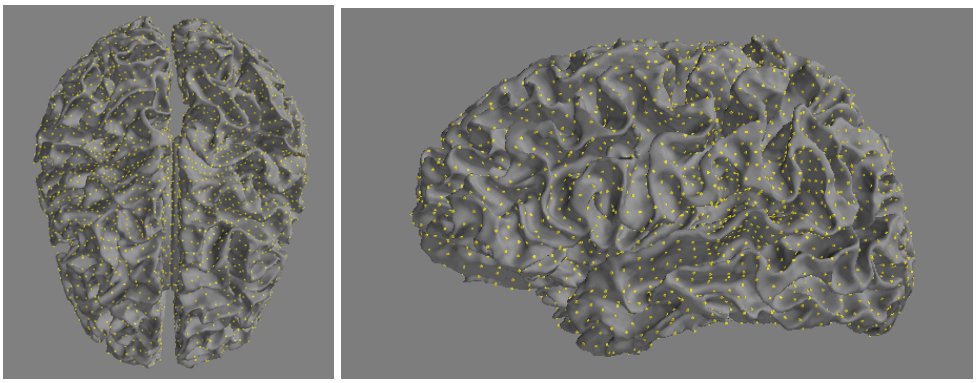

**Figure 12 and 13**: Surface-based source space example

- Forward operator

Now, the forward operator can be computed by using a simple command-line *mne.make_forward_solution()* and introducing the following inputs:

- Trans file.
- Source space.
- BEM model.
- Info attribute.

### 5.2.5. Inverse Solution

Once the forward operator has been computed, we can move forward to the computation of the inverse operator. This operator has to be applied to the evoked or epochs data container to estimate the active sources.

The inverse operator is computed by calling the MNE function *make_inverse_operator()* and introducing the following inputs:

- Info attribute.
- Forward operator.
- Noise-covariance matrix.

The estimated sources are defined in the source space.

Finally, in order to actually locate the sources, several different unique solutions to the ill-posed electromagnetic inverse problem exist. MNE provides a wide selection of inverse modelling approaches. The decision of which method should be used is discussed in the next section.

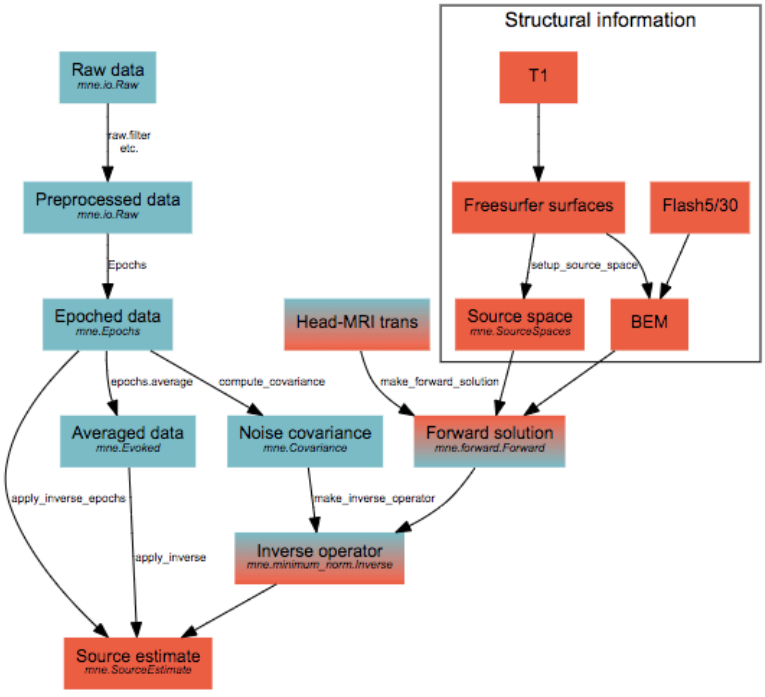


**Figure 14**: Workflow of the MNE software.[6]

## 5.3. Results

This section discuses which method should be used in order to solve the inverse problem and how we computed the validation of the model after performing the pipeline mentioned before. Also,

presents the obtained results with an explanation on how the localization of the active sources was determined.

### 5.3.1. Method selected

The pipeline presented in the latter section was used for every subject of the two groups, control and encephalitic. As stated before, MNE provides a wide selection on inverse modelling approaches. Moreover, each localization technique has its own modelling assumptions and thus strengths and limitations. These different possible approaches in MNE are dSPM, MNE, sLORETA, and eLORETA. During the evaluation of each subject, all inverse modelling approaches were used in order to observe which method performed best.

In [38] it was stated that there is not an straight answer toward the question of which method is "best". Therefore, in order to decide which localization method needed to be used, several premises where considered. First, it was taken into account that dSPM and sLORETA have lower localization error than MNE. [39] Secondly, when computing these methods in MNE, it was observed that each approach has a respective explained variance, and this is a good indicative of which method performs best. Finally, since the inverse problem applied to EEG is a well-studied problem, the criteria applied in similar studies from recent literature was considered.

Once the code was run for every subject, it was observed that there was no difference regarding the explained variance between dSPM, MNE and sLORETA methods. However, the explained variance in eLORETA was, usually, lower than for the other methods. Due to these results, eLORETA was no longer considered as a possible modelling approach. Finally, it was taken into account the criteria used in [6] and in [38] , since they performed a similar analysis as the one presented here. Thereby, it was decided that the method that would be applied to the inverse operator would be dSPM.

### 5.3.2. Model validation

The validation was computed at IDIBAPS research center by Heike Stein and Albert Compte, experts in the Theoretical Neurobiology and Computational Neuroscience fields. The validation of the model was possible since there were some regions of the brain that were expected to be activated at concrete times of the trial.

These two regions were the occipital region and the parietal region. The occipital lobe is related with the visual activity of the subject, whereas the parietal lobe (motor cortex) is related with the movements of the subject. During the trial, it was expected to observe the occipital lobe activated when the dot (stimulus) was presented to the patient. Additionally, the parietal lobe was expected

to be activated when the participant moved the mouse. Also, since all the patients were right-handed, it was expected that this activity was reflected in the left hemisphere which is related with the right movements. [40]

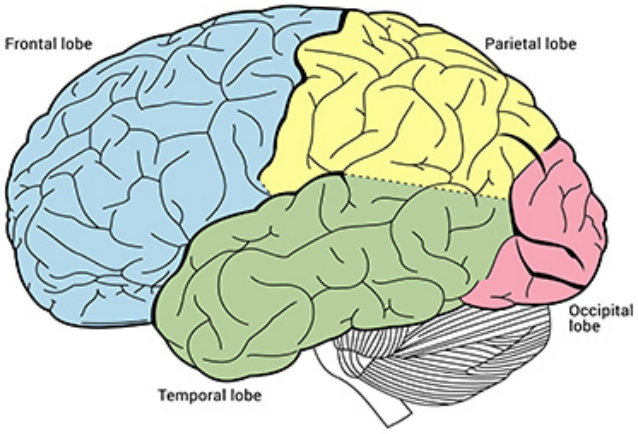


**Figure 15**: Brain lobes [61]

In order to compute the validation, two files respepoch and longepoch were analysed. As mentioned before, the respepoch file was centered (time = 0s) at that moment the participant was moving the mouse. On the other hand, the longepoch file was centered when the visual stimulus was presented. Therefore, it was expected to observe at time 0 a motor activity in the respeoch data analysis, and an occipital activity in the longepoch analysis.

The approach undertaken to compute the validation consisted in creating a new subject which was the average of all controls. The head model for this new subject was created with a subject already provided by FreeSurfer which represents an average reconstruction of all the reconstructions computed by FreeSurfer. FreeSurfer creates the new subject automatically and is updated as reconstructions are made.

The results obtained can be observed in figures 16 and 17. Both figures show the presence of brain activity at time 0 s. The EEG data of 16 and 17 represented an average of the electrical activity found in the longepochs and respeoch files, respectively. First, in 16 it is depicted the left hemisphere of the patient, and it can be observed that the occipital lobe is activated. On the other hand, in 17 it can be observed the left hemisphere of the patient and an activation in the parietal lobe. Consequently, the model was validated since it showed promising results which were anatomically significant. It is important to state that other regions might be activated. Nevertheless, the model can still be validated, as long as the regions of interest are activated.

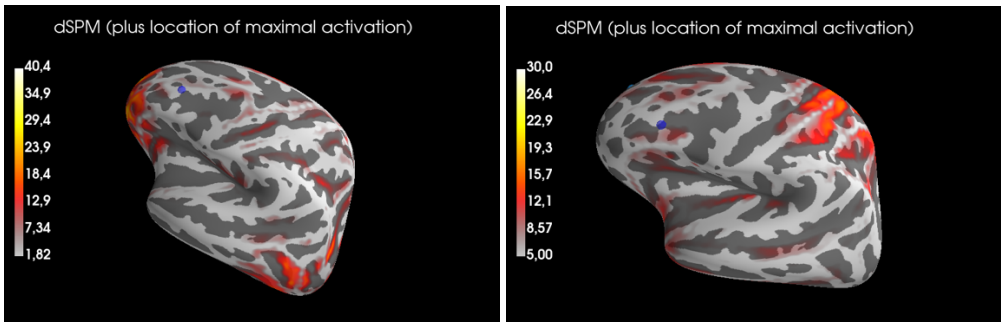


**Figures 16 and 17**: 16 represents the longepoch result (t=0s) and 17 represents the respeoch results (t=0s)

### 5.3.3. Final Results

The main objective of this project consisted in localizing specific brain regions at a concrete time of the trial. Therefore, the approach considered to achieve this goal, consisted in localizing all the activated regions for every patient and try to find a pattern in the different groups.

The particular time we wanted to observe was located instants before the visual stimulus was shown to the patients. More specifically, when using the longepoch files, the time of interest was located between [-1,-0.8] seconds.

After the validation of the model, the code was run for every subject and all the activated regions found during the time of interest were recorded. This recorded information were the x, y and z coordinates of the localized source.

It was observed that all subjects showed more than one region activated per hemisphere. In order to find a certain correlation between all the locations found, different datasets were created. These datasets contained the localization coordinates found in every subject. There were four datasets, one for the coordinates of the sources located in the left hemisphere of the control subject; another for the right hemisphere of this group; and two more for the different hemispheres of the encephalitic group. Then, a Principal Component Analysis was applied to the different databases, and a plot of the first two principal components was evaluated. PCA allowed to increase the interpretability of our datasets. It was found that practically 90% of the information of the original dataset was found in the first two principal components. Thereby, it was considered that the plots of the first two principal components (PCs) allowed us to observe possible correlations between the different observations.

The results obtained showed that there seemed to be certain correlation between some sources found in the left hemisphere in the control and right hemisphere of the encephalitic group. However, the results obtained from the PCA containing the data of the right hemisphere of the control group and the left hemisphere of the encephalitic group did not show any concrete a pattern followed by

the different participants. These results can be found in the annexes (12.3). It is important to state the fact that a pattern was considered to be found if at least four participants shared a cluster in the PCA plot. If this threshold was accomplished, it meant that at approximately 50% of the participants in the two groups had similar information.

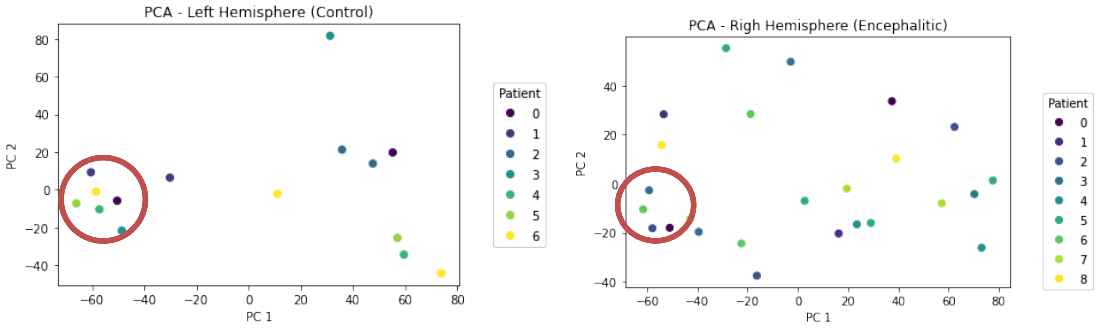


**Figure 18 and 19**: 18 and 19 depict the first two PCs and considered clusters for the source coordinates of the left and right hemispheres in Control and Encephalitic Group, respectively

Figure 18 shows a clear cluster composed by all the participants of the control group. The mean and standard deviation of the coordinates corresponding to these observations was computed. On the other hand, figure 19 (encephalitic) did not show a pattern as clear as in the Control group. However, the cluster considered is depicted in the plot. The chosen cluster was selected since was the cluster which contained the highest number of participants and satisfied the established threshold conditions. Again, the mean and standard deviation corresponding to the coordinates of these observations was calculated. The final results are presented in the following table:

| Group | Mean | Standard Deviation |
|---|---|---|
| Control | (-21.47, 48.45, 15.4) | (9.64, 8.93, 18.73) |
| Encephalitic | (38.38, -65.96, 2.82) | (3.94, 8.9, 5.62) |

**Table 4**: Mean and standard deviation of the localized sources in control and encephalitic groups.

The results obtained revealed that all subjects in the control group shared a specific source located at the left hemisphere with a coordinate mean of (-21.47, 48.45, 15.4) $\pm$ (9.64, 8.93, 18.73). Whereas, in the case of the encephalitic group, 4 patients out of 9, showed a specific source at the right hemisphere with a coordinate mean of (38.38, -65.96, 2.82) $\pm$ (3.94, 8.9, 5.62).

In the anatomical point of view, the coordinates found in the control group correspond to the frontal lobe of the brain, and the coordinates regarding the encephalitic group correspond to the temporal lobe and part of the occipital lobe of the right hemisphere.

Figures 20 and 21 show the activity of a control subject and an encephalitic subject instants before the trial Figure 20 depicts at the frontal lobe of the left hemisphere the activated sources of a specific

control subject (subject 4). In Figure 21 it can be observed the right hemisphere of a subject from the encephalitic group (subject 7). It can be observed that the active sites are located in the temporal lobe and part of the occipital lobe of the patient.

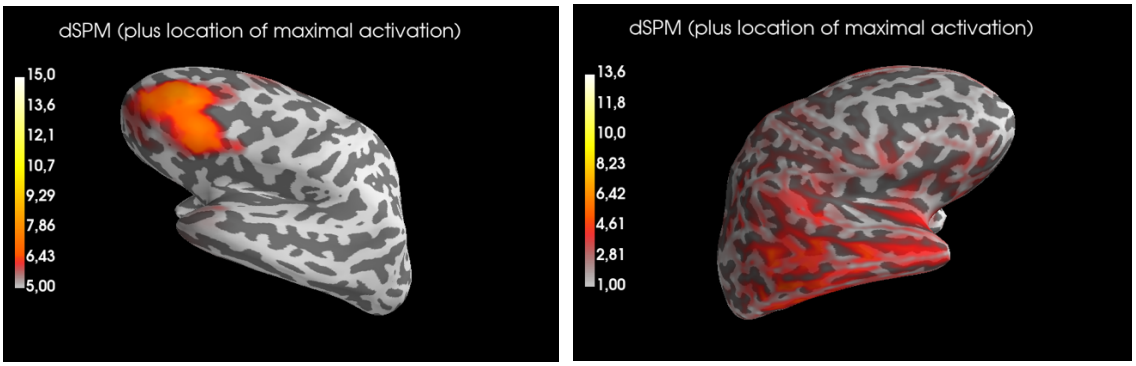


**Figure 20 and 21**: Control 4 and encephalitic 7 sources of activation at time -0.9s.

Despite it has been possible to find certain patterns between the individuals of this study, it is important to remark the fact that this project was carried out with very few participants. It is greatly important not to fall under false assumptions and consider that these results can be generalized to any healthy or encephalitic person. However, the results obtained are very promising, and the code implemented should be repeated once more data is acquired from different subjects.

### 5.3.4. Discussion

The results obtained in the latter section were able to establish certain differences between the Anti-NMDAR encephalitic patients and the control group. These results corroborate the results obtained at the IDIBAPS research group headed by Albert Compte. It has been observed that instants before the visual stimulus, the activated sites between control groups and encephalitic groups differ. In the case of the control group, the activated region is located at the frontal lobe of the left hemisphere. Whereas, in the case of the encephalitic group the activated region is located at the temporal lobe of the right hemisphere.

In [41], EEG analysis using independent component analysis detected that the left hemisphere of Anti-NMDAR encephalitic patients had intermittent slowing waves. Also, in [41] it was reported that the EEG of Anti-NMDAR encephalitic patients revealed slow-wave activity in 82.4% patients. The findings in [41] and [42] could explain the results obtained in this project and clarify the differences observed among the two groups. It could be possible that the activation of the left hemisphere in the encephalitic patients took place a few seconds after since the propagation of the wave is slower. On the other hand, the studies [43] and [44], have reported brain abnormalities in patients with Anti-NMDAR detected throughout MRI findings; abnormal T2/Flair hyperintense signals were detected in the temporal/occipital lobes. It might be possible, that these anatomical alterations could explain

the activity found in the right hemisphere of the encephalitic group at the temporal/occipital lobes. However, further studies in this area should be conducted in order to confirm this hypothesis.

Although the studies mentioned above might provide promising arguments to justify the results obtained in this project, there are many limitations that should be taken into account. For instance, the conditions between the studies were very different, none of these studies conducted memory task trials. Also, there is a high variability between the different participants that participated in the studies, for example it should be taken into account the number of patients, the biological sex, the ages, the state of the diseases, and many other factors which are highly relevant. Acknowledging the differences and similarities among the different studies might allow us to confirm if their conclusions could be considered as possible explanations of the results obtained in this study.

On the other hand, it is worth mentioning the implications these results have provided to the IDIBAPS research group. This project has enabled to localize the sources that originate the differences in the electrical activity recorded in an EEG during a working memory trial. However, Compte and his group had also demonstrated that in the frequency space, the differences were located at a concrete frequency bandwidth which was alpha. In this project, all the frequencies of the EEG have been considered and, therefore, the sources localized were not specifically coming from alpha. Future lines of investigation could imply repeating this project but by filtering the alpha frequency and, then finding the sources which are only related to alpha.

.

## 6. EXECUTION PLAN

In figure 22, the GANTT graph of the project is presented. This graph has been very useful in order to control the schedules established for each task. The entire project was divided into five phases which were completed by the end of six months.

| Phase | Task | Hours | January | | | | February | | | | March | | | | April | | | | May | | | | June | | | |
|---|---|---|---|---|---|---|---|---|---|---|---|---|---|---|---|---|---|---|---|---|---|---|---|---|---|---|
| | | | 1 | 2 | 3 | 4 | 1 | 2 | 3 | 4 | 1 | 2 | 3 | 4 | 1 | 2 | 3 | 4 | 1 | 2 | 3 | 4 | 1 | 2 | 3 | 4 |
| 1 | Study inverse problem applied in EEG. | 18 | | | X | X | | | | | | | | | | | | | | | | | | | | |
| | Analysis of programming envrionments. | 23 | | | | X | X | | | | | | | | | | | | | | | | | | | |
| 2 | Installation and familiarization: FreeSurfer and MNE-Python. | 7 | | | | | | X | | | | | | | | | | | | | | | | | | |
| | Study of examples and tutorials. | 12,5 | | | | | | X | X | | | | | | | | | | | | | | | | | |
| | Pipline development | 35 | | | | | | | X | X | | | | | | | | | | | | | | | | |
| 3 | Testing, modifying, and applying the code. | 65 | | | | | | | | | X | X | X | X | | | | | | | | | | | | |
| 4 | Validation of the model | 4 | | | | | | | | | | | | | X | | | | | | | | | | | |
| 5 | Run the model for every patient. | 75 | | | | | | | | | | | | | X | X | X | X | X | | | | | | | |
| | Statistical analysis. | 10 | | | | | | | | | | | | | | | | | | X | X | | | | | |
| 6 | Final Report. | 39 | | | | | | | | | | | | | | | | | | | X | X | X | X | | |
| | Preparation presentation. | 12 | | | | | | | | | | | | | | | | | | | | | | X | X | |
| | Final presentation. | 0,5 | | | | | | | | | | | | | | | | | | | | | | | X | |

**Figure 22**: GANTT graph of the project

# 7. TECHNICAL FEASIBILITY

In this section, it is examined the SWOT analysis regarding the project. The strength, weaknesses, opportunities, and threats are presented.

Strengths: MNE is an open-source software package, therefore, not only the package itself is free, but the working environment is also open-source. In the case of other open-source packages, such as FieldTrip, EEGLAB or Brainsotm, they came with the downside that depended on expensive commercial programming environments. [6,34–36] On the other hand, it is worth mentioning that the principal developer of this project had previous experience working in the Python environment. On the other hand, this working environment offers flexibility, and the code can be adapted to the user's preferences.

Weaknesses: As stated before, the main weakness of this project was the limited amount of time and the limited amount of data. Regarding the amount of data, it is important to mention that many models which aim in establishing a generalized criterion suffers from a lack of data. Also, since the EEG data and MRI data are sensitive to noise, it is possible that some observations are affected due to instrumental and/or environmental noise. More concretely, EEG technique is highly susceptible to various forms and sources of noise, which present significant difficulties and challenges in analysis and interpretation of EEG data. On the other hand, several challenges are faced regarding the complexity of the datasets in brain science. [45] For instance, data might come unstructured, heterogeneous, and generated from different sources which makes it difficult to interpret and process.

Opportunities: The main opportunity of this project is the fact that, nowadays, we are facing the era of big data and brain science is a fast-developing field. Brain science has entered a new era of big data with the development of new tools for mapping neuronal connections, the increasing resolution of imaging technologies, and the explosion of nanoscience. [45]

Threats: In the medical field and more concretely in the neuroscience field, this diversity among participants might become a beneficial, since the subjects in a research should reflect the diversity of our culture and conditions, taking into account race, ethnicity, biological sex, age etc. [46] However, as it has been previously mentioned, it is difficult to fulfil the requisite of the ideal number of patients. Although the patients in this came from different countries, all of them were European or from the United Kingdom, none of them came from an ethnic and racial minority. A lot of work needs to be done to represent these minorities in clinical trials/research since the medical product and treatments will be ultimately used by the general population.

# 8. ECONOMICAL FEASIBILITY

Furthermore, considering the total time inverted, the required data needed for the execution of the project, and the different technicians involved in the project, it is needed to establish an approximate total budget of the project.

In order to execute the project, two medical images/signals are needed:

| Technique | Cost (€/unit) | Time (min/unit) |
|---|---|---|
| MRI | 125 [62] | 85 |
| EEG | 100 [63] | 90 |

**Table 5:** Cost and time required for an MRI and EEG exam

On the other hand, there was a total number of X patients:

| Group | Number of subjects | Technique(s) | Total Cost (€/group) |
|---|---|---|---|
| Control group | 7 | MRI,EEG | 1,575 |
| Anti-NMDAR | 9 | MRI,EEG | 2,025 |
| Total cost of data acquisition | | | 3,600 |

**Table 6:** Cost of data acquisition and cost for each group

Regarding the human resources that participated in this project, a data acquisition technician was needed in order to acquire the MRI and EEG data of all patients. The cost of this technician was estimated to be approximately 23 €/hour [64]. On the other hand, besides from the principal developer (biomedical engineer student), it was needed to have a tutor who would lead and advice the developer. The cost of the student can be estimated by considering the annual salary of a junior engineer, which is approximately 20€/hour [65]. The cost of the tutor can be estimated by considering the salary of a senior engineer, which is approximately 30 €/hour [65]. Finally, it is essential for the student to have a computer for the entire development of the project.

| Technicians + equipment | Total time inverted (hours) | Cost (€ / hour) | Total Cost (€) |
|---|---|---|---|
| Data acquisition technician | 47 | 23 | 1,081 |
| Student | 300 | 20,0 | 6,000 |
| Tutor/Director | 80 | 30,0 | 2,400 |
| MacBook Pro (13-inch),2019 | - | - | 1,575 |
| Total cost: | | | 11,056 |

**Table 7** Technicians and equipment budget

Considering the results obtained in the latter tables, it can be approximated a total budget for the project of **14,656 €**.

# 9. REGULATION AND LEGAL ASPECTS

Legal aspects were taken into account during the whole development of the project in order to ensure all time a correct and secure investigation. This project was under the regulations established by Universitat de Barcelona *Normes generals reguladores dels treballs de fi de grau de la Universitat de Barcelona* [66]. More precisely, the regultation *Normes reguladores dels treballs de fi de grau del grau en enginyeria biomèdica de la Universitat de Barcelona* [67], which correspond to specific regulations of the biomedical engineering degree at Universitat de Barcelona.

Moreover, considering the fact that this project implied working with data extracted from patients, it is essential to ensure data protection. Data and digital rights are protected under the regulation *Ley Orgánica 3/2018, de 5 de diciembre, de Protección de Datos Personales y garantía de los derechos digitales*. [68] This latter regulation reckons with some key points found in the European regulation General Data Protection 2016/679 (GDPR). All data has been collected with the appropriate consent from the patients and has been treated anonymously to ensure the intimacy and rights of the patients.

Finally, the regulation *Ley 14/2011, de 1 de junio, de la Ciencia, la Tecnoogía y la Innovación* [69] presents some key points for the rights and duties of the researches (articles 14 and 15, respectively) in any scientific investigation. This regulation recognized the rights of the researches by acknowledging their authorship in all the scientific projects that the researcher has taken part in.

## 10. CONCLUSIONS AND FUTURE LINES

In conclusion, this project has accomplished the objective of creating an appropriate source reconstruction algorithm by using the MNE-Python software package. This algorithm is capable of solving the ill-posed inverse problem and localize the brain regions that give rise to electrical activity recorded at the scalp during an EEG recording.

Thanks to the collaboration of experts in the fields of theoretical neurobiology and computational neuroscience, the algorithm was validated. It has also been possible to define a pipeline containing the practical steps that need to be followed when computing the EEG source localization in the MNE-Python package.

It has been observed that besides MNE-Python there exist several powerful commercial and academic packages capable of performing the EEG source imaging. It has been discussed that the decision regarding which software performs best is unknown and depends on the preferences and judgment of the programmer.

Also, this project has illustrated some of the future lines of research the EEG source reconstruction could take part in. Additionally, in the areas of Brain Computing Interface, Epilepsy, and hyperscanning, EEG source reconstruction has demonstrated to have an essential role in their current and future developments.

In light of the results obtained, it has been possible to characterize the anatomical regions that produce electrical differences among encephalitic groups and control groups during a working memory trial. It has been observed that some control subjects shared an active area located at the frontal lobe of the left hemisphere. Whereas, when analysing trial in the encephalitic subjects, it was observed that the active source was located at the right hemisphere at the temporal/occipital lobes. This analysis was performed by examining a concrete moment of the trial, which took place instants before the visual stimulus was shown to the patients.

It is worth mentioning that although the results obtained in this project are very promising, more studies in this field need to be conducted. Further analysis needs to be done in order to obtain more accurate and reliable results. The future lines of investigation of this project and in all the fields in medicine, relay on the multidisciplinary collaboration among physicians, biomedical engineers, researches and data scientists. It is greatly important to endorse the work among these disciplines so the advances in treatment and diagnosis go towards the principles of minimally invasive procedures, personalized medicine, and medical ethics.

# 11. REFERENCES


1. Michel CM, Murray MM. Towards the utilization of EEG as a brain imaging tool. NeuroImage [Internet]. 2012;61(2):371–85. Available from: http://dx.doi.org/10.1016/j.neuroimage.2011.12.039
2. Cline CC, Coogan C, He B. EEG electrode digitization with commercial virtual reality hardware. PLoS ONE. 2018;13(11):1–13.
3. Song J, Davey C, Poulsen C, Luu P, Turovets S, Anderson E, Li K, Tucker D. EEG source localization: Sensor density and head surface coverage. Journal of Neuroscience Methods [Internet]. 2015;256:9–21. Available from: http://dx.doi.org/10.1016/j.jneumeth.2015.08.015
4. Grech R, Cassar T, Muscat J, Camilleri KP, Fabri SG, Zervakis M, Xanthopoulos P, Sakkalis V, Vanrumste B. Review on solving the inverse problem in EEG source analysis. Journal of NeuroEngineering and Rehabilitation. 2008;5:1–33.
5. Liu Z, Ding L, He B. Integration of EEG/MEG with MRI and fMRI. IEEE Engineering in Medicine and Biology Magazine. 2006;25(4):46–53.
6. Gramfort A, Luessi M, Larson E, Engemann DA, Strohmeier D, Brodbeck C, Goj R, Jas M, Brooks T, Parkkonen L, Hämäläinen M. MEG and EEG data analysis with MNE-Python. Frontiers in Neuroscience. 2013;7(7 DEC):1–13.
7. Fischl B. FreeSurfer. NeuroImage. 2012;62(2):774–81.
8. Gramfort A, Luessi M, Larson E, Engemann DA, Strohmeier D, Brodbeck C, Parkkonen L, Hämäläinen MS. MNE software for processing MEG and EEG data. NeuroImage [Internet]. 2014;86:446–60. Available from: http://dx.doi.org/10.1016/j.neuroimage.2013.10.027
9. Apartados Básicos Memoria Proyectos TFG : Grado en Ingeniería Biomédica. 2020;9:2020.
10. st. Louis E, Frey L, Britton J, Hopp J, Korb P, Koubeissi M, Lievens W, Pestana-Knight E. Electroencephalography (EEG): An Introductory Text and Atlas of Normal and Abnormal Findings in Adults, Children, and Infants. Electroencephalography (EEG): An Introductory Text and Atlas of Normal and Abnormal Findings in Adults, Children, and Infants. 2016.
11. Rashid M, Sulaiman N, P. P. Abdul Majeed A, Musa RM, Ahmad AF, Bari BS, Khatun S. Current Status, Challenges, and Possible Solutions of EEG-Based Brain-Computer Interface: A Comprehensive Review. Frontiers in Neurorobotics. 2020;14(June):1–35.
12. Ledwidge P, Foust J, Ramsey A. Recommendations for Developing an EEG Laboratory at a Primarily Undergraduate Institution. Journal of undergraduate neuroscience education : JUNE : a publication of FUN, Faculty for Undergraduate Neuroscience [Internet]. 2018;17(1):A10–9. Available from: http://www.ncbi.nlm.nih.gov/pubmed/30618494%0Ahttp://www.pubmedcentral.nih.gov/articlerender.fcgi?artid=PMC6312138
13. Wendel K, Väisänen O, Malmivuo J, Gencer NG, Vanrumste B, Durka P, Magjarević R, Supek S, Pascu ML, Fontenelle H, Grave De Peralta Menendez R. EEG/MEG source imaging: Methods, challenges, and open issues. Computational Intelligence and Neuroscience. 2009;2009.
14. Seeck M, Koessler L, Bast T, Leijten F, Michel C, Baumgartner C, He B, Beniczky S. The standardized EEG electrode array of the IFCN. Clinical Neurophysiology [Internet]. 2017;128(10):2070–7. Available from: http://dx.doi.org/10.1016/j.clinph.2017.06.254
15. Beniczky S, Schomer DL. Electroencephalography: basic biophysical and technological aspects important for clinical applications. Epileptic Disorders. 2020;22(6):697–715.
16. Consumo MDESY. Resonancia magnética con magnetos de 3 teslas. 2006.
17. Vatta F, Meneghini F, Esposito F, Mininel S, di Salle F. Realistic and spherical head modeling for EEG forward problem solution: A comparative cortex-based analysis. Computational Intelligence and Neuroscience. 2010;2010.

18. Phillips C, Rugg MD, Friston KJ. Anatomically informed basis functions for EEG source localization: Combining functional and anatomical constraints. NeuroImage. 2002;16(3 I):678–95.
19. Fuchs M, Wagner M, Kastner J. Boundary element method volume conductor models for EEG source reconstruction. Clinical Neurophysiology. 2001;112(8):1400–7.
20. Hallez H, Vanrumste B, Grech R, Muscat J, de Clercq W, Vergult A, D'Asseler Y, Camilleri KP, Fabri SG, van Huffel S, Lemahieu I. Review on solving the forward problem in EEG source analysis. Journal of NeuroEngineering and Rehabilitation. 2007;4.
21. Michel CM, Brunet D. EEG source imaging: A practical review of the analysis steps. Frontiers in Neurology. 2019;10(APR).
22. Asadzadeh S, Yousefi Rezaii T, Beheshti S, Delpak A, Meshgini S. A systematic review of EEG source localization techniques and their applications on diagnosis of brain abnormalities. Journal of Neuroscience Methods. 2020;339:1–23.
23. Ens E, Inria U, Clerc M, Keriven R. Imaging Methods for MEG / EEG Inverse Problem. (4).
24. Lopez Rincon A, Shimoda S. The inverse problem in electroencephalography using the bidomain model of electrical activity. Journal of Neuroscience Methods [Internet]. 2016;274:94–105. Available from: http://dx.doi.org/10.1016/j.jneumeth.2016.09.011
25. Jan D. Online Workshop on EEG Data Processing with MNE - Phyton. 2021;(May).
26. Sohrabpour A, Cai Z, Ye S, Brinkmann B, Worrell G, He B. Noninvasive electromagnetic source imaging of spatiotemporally distributed epileptogenic brain sources. Nature Communications [Internet]. 2020;11(1). Available from: http://dx.doi.org/10.1038/s41467-020-15781-0
27. Luu TP, Nakagome S, He Y, Contreras-Vidal JL. Real-time EEG-based brain-computer interface to a virtual avatar enhances cortical involvement in human treadmill walking. Scientific Reports [Internet]. 2017;7(1):1–12. Available from: http://dx.doi.org/10.1038/s41598-017-09187-0
28. van Mierlo P, Vorderwülbecke BJ, Staljanssens W, Seeck M, Vulliémoz S. Ictal EEG source localization in focal epilepsy: Review and future perspectives. Clinical Neurophysiology. 2020;131(11):2600–16.
29. Kaiboriboon K, Lüders HO, Hamaneh M, Turnbull J, Lhatoo SD. EEG source imaging in epilepsyĝ€"practicalities and pitfalls. Nature Reviews Neurology. 2012;8(9):498–507.
30. Czeszumski A, Eustergerling S, Lang A, Menrath D, Gerstenberger M, Schuberth S, Schreiber F, Rendon ZZ, König P. Hyperscanning: A Valid Method to Study Neural Inter-brain Underpinnings of Social Interaction. Frontiers in Human Neuroscience. 2020;14(February):1–17.
31. Liu D, Liu S, Liu X, Zhang C, Li A, Jin C, Chen Y, Wang H, Zhang X. Interactive brain activity: Review and progress on EEG-based hyperscanning in social interactions. Frontiers in Psychology. 2018;9(OCT):1–11.
32. Stefan H, Trinka E. Magnetoencephalography (MEG): Past, current and future perspectives for improved differentiation and treatment of epilepsies. Seizure [Internet]. 2017;44:121–4. Available from: http://dx.doi.org/10.1016/j.seizure.2016.10.028
33. Stefan H, Trinka E. Magnetoencephalography (MEG): Past, current and future perspectives for improved differentiation and treatment of epilepsies. Seizure [Internet]. 2017;44:121–4. Available from: http://dx.doi.org/10.1016/j.seizure.2016.10.028
34. Baillet S, Friston K, Oostenveld R. Academic software applications for electromagnetic brain mapping using MEG and EEG. Vol. 2011, Computational Intelligence and Neuroscience. 2011.
35. Tadel F, Baillet S, Mosher JC, Pantazis D, Leahy RM. Brainstorm: A user-friendly application for MEG/EEG analysis. Computational Intelligence and Neuroscience. 2011;2011.

36. Oostenveld R, Fries P, Maris E, Schoffelen JM. FieldTrip: Open source software for advanced analysis of MEG, EEG, and invasive electrophysiological data. Computational Intelligence and Neuroscience. 2011;2011.
37. Quick Start : Installing Python and Packages. :3.
38. Jas M, Larson E, Engemann DA, Leppäkangas J, Taulu S, Hämäläinen M, Gramfort A. A reproducible MEG/EEG group study with the MNE software: Recommendations, quality assessments, and good practices. Frontiers in Neuroscience. 2018;12(AUG):1–18.
39. Wei C, Lou K, Wang Z, Zhao M, Mantini D, Liu Q. Edge Sparse Basis Network: A Deep Learning Framework for EEG Source Localization. 2021; Available from: http://arxiv.org/abs/2102.09188
40. Hand F. Fact Sheet Right Brain , Left Brain :
41. Meixensberger S, Tebartz van Elst L, Schweizer T, Maier SJ, Prüss H, Feige B, Denzel D, Runge K, Nickel K, Matysik M, Venhoff N, Domschke K, Urbach H, Perlov E, Endres D. Anti-N-Methyl-D-Aspartate-Receptor Encephalitis: A 10-Year Follow-Up. Frontiers in Psychiatry. 2020;11(May):1–9.
42. Yang S, Yang L, Liao H, Chen M, Feng M, Liu S, Tan L. Clinical Characteristics and Prognostic Factors of Children With Anti-N-Methyl-D-Aspartate Receptor Encephalitis. Frontiers in Pediatrics. 2021;9(April).
43. Jesús SN de, Yudit MR. Encefalitis sinápticas autoinmunes. 2011;
44. Yu Y, Wu Y, Cao X, Li J, Liao X, Wei J, Huang W. The Clinical Features and Prognosis of Anti-NMDAR Encephalitis Depends on Blood Brain Barrier Integrity. Multiple Sclerosis and Related Disorders. 2021;47.
45. Qu H, Lei H, Fang X. Big Data and the Brain: Peeking at the Future. Genomics, Proteomics and Bioinformatics [Internet]. 2019;17(4):333–6. Available from: https://doi.org/10.1016/j.gpb.2019.11.003
46. Clark LT, Watkins L, Piña IL, Elmer M, Akinboboye O, Gorham M, Jamerson B, McCullough C, Pierre C, Polis AB, Puckrein G, Regnante JM. Increasing Diversity in Clinical Trials: Overcoming Critical Barriers. Current Problems in Cardiology. 2019;44(5):148–72.
47. East Neurology. 2021. EEG: brain wave test - East Neurology. [online] Available at: <https://eastneurology.com.au/eeg-electroencephalogram-brain-wave-tests/> [Accessed 13 June 2021].
48. TruScan EEG | DEYMED Diagnostic. [online] DEYMED Diagnostic - Neurodiagnostic EEG, EMG, PSG & TMS devices. Available at: <https://deymed.com/truscan-eeg> [Accessed 13 June 2021].
49. Neuroelectrics: Reinventing brain health. 2021. [online] Available at: <https://www.neuroelectrics.com/solutions/enobio> [Accessed 13 June 2021].
50. En.wikipedia.org. 2021. 10–20 system (EEG) - Wikipedia. [online] Available at: <https://en.wikipedia.org/wiki/10%E2%80%9320_system_(EEG)> [Accessed 13 June 2021].
51. (ACR), R., 2021. Magnetoencephalography. [online] Radiologyinfo.org. Available at: <https://www.radiologyinfo.org/en/info/meg> [Accessed 13 June 2021].
52. Mne.tools. 2021. Source localization with MNE/dSPM/sLORETA/eLORETA — MNE 0.23.0 documentation. [online] Available at: <https://mne.tools/stable/auto_tutorials/inverse/30_mne_dspm_loreta.html> [Accessed 13 June 2021].
53. Mne.tools. 2021. Head model and forward computation — MNE 0.23.0 documentation. [online] Available at: <https://mne.tools/stable/auto_tutorials/forward/30_forward.html#tut-forward> [Accessed 13 June 2021].

54. Mne.tools. 2021. Plotting EEG sensors on the scalp — MNE 0.23.0 documentation. [online] Available at: <https://mne.tools/stable/auto_examples/visualization/eeg_on_scalp.html#sphx-glr-auto-examples-visualization-eeg-on-scalp-py> [Accessed 13 June 2021].
55. Mne.tools. 2021. Compute MNE-dSPM inverse solution on evoked data in volume source space — MNE 0.23.0 documentation. [online] Available at: <https://mne.tools/stable/auto_examples/inverse/compute_mne_inverse_volume.html> [Accessed 13 June 2021].
56. Mne.tools. 2021. Glossary — MNE 0.23.0 documentation. [online] Available at: <https://mne.tools/stable/glossary.html> [Accessed 13 June 2021].
57. Mne.tools. 2021. The Info data structure — MNE 0.23.0 documentation. [online] Available at: <https://mne.tools/stable/auto_tutorials/intro/30_info.html> [Accessed 13 June 2021].
58. Mne.tools. 2021. Working with sensor locations — MNE 0.23.0 documentation. [online] Available at: <https://mne.tools/stable/auto_tutorials/intro/40_sensor_locations.html> [Accessed 13 June 2021].
59. Mne.tools. 2021. Setting the EEG reference — MNE 0.23.0 documentation. [online] Available at: <https://mne.tools/stable/auto_tutorials/preprocessing/55_setting_eeg_reference.html> [Accessed 13 June 2021].
60. Mne.tools. 2021. Installing MNE-Python — MNE 0.23.0 documentation. [online] Available at: <https://mne.tools/stable/install/mne_python.html> [Accessed 13 June 2021].
61. Qbi.uq.edu.au. 2021. Lobes of the brain. [online] Available at: <https://qbi.uq.edu.au/brain/brain-anatomy/lobes-brain> [Accessed 13 June 2021].
62. Smartsalus.com. 2021. Desde 90€ Resonancia Magnética - RMN en Barcelona. [online] Available at: <https://www.smartsalus.com/barcelona/radiologia/resonancia-magnetica-rmn> [Accessed 13 June 2021].
63. Smartsalus.com. 2021. 75€ Electroencefalograma en Barcelona. [online] Available at: <https://www.smartsalus.com/barcelona/electroencefalograma-o-eeg-en-barcelona-3063> [Accessed 13 June 2021].
64. Castillo, E., 2020. Analista De Datos, El Puesto Más Demandado (Y Mejor Pagado) Por Las Empresas. [online] Cinco Días. Available at: <https://cincodias.elpais.com/cincodias/2018/04/09/midinero/1523274767_631043.html> [Accessed 13 June 2020].
65. Boe.es. 2021. [online] Available at: <https://www.boe.es/boe/dias/2019/03/01/pdfs/BOE-A-2019-2956.pdf> [Accessed 13 June 2021].
66. Ub.edu. 2020. [online] Available at: <https://www.ub.edu/portal/documents/4493882/5180729/normes_TFG.pdf/63abc3a2-27ce-8dbd-4463-80e1662ee21d> [Accessed 13 June 2021].
67. Ub.edu. 2021. Grado de Ingeniería Biomédica - Facultat de Medicina y Ciencias de la Salud - Universidad de Barcelona. [online] Available at: <https://www.ub.edu/portal/web/medicina-ciencias-salud/grados/-/ensenyament/detallEnsenyament/6178758/10> [Accessed 13 June 2021].
68. Boe.es. 2020. BOE.Es - Documento Consolidado BOE-A-2018-16673. [online] Available at: <https://www.boe.es/buscar/act.php?id=BOE-A-2018-16673> [Accessed 7 June 2020].
69. Boe.es. 2020. BOE.Es - Documento Consolidado BOE-A-2011-9617. [online] Available at: <https://www.boe.es/buscar/act.php?id=BOE-A-2011 9617&tn=1&p=20200318> [Accessed 13 June 2021].

# 12. ANNEXES

## 12.1. FreeSurfer – Anatomical MRI reconstruction

Name of the folder in which one can find the FreeSurfer software*: freesurfer*
Name of the folder which contains all slices of the anatomical MRI (the slices are files which are named from 0 to 207, each file represents a concrete slice): *MRI*
Name of the folder which contains a folder for each subject with the final reconstruction results: *subjects_group*
Name of the subject that we want to create inside *subjects_group*: SUB01 (example).
Steps for performing the reconstruction:

1. Open terminal.
2. Insert the command: *FREESURFER_HOME=/User/freesurfer*
3. Insert the command*: SUBJECTS_DIR=/User/subjects_group*
4. Insert the command: *$FREESURFER_HOME/FreeSurferSetUp.sh*
5. Insert the command: recon-all -s SUB01 -I /User/MRI/0

In recon-all it is only needed to indicate the location of one of the slices obtained during the MRI, with this information FreeSurfer is capable of finding the remaining slices. This command needs a lot of time, approximately between 8-14 hours.

## 12.2. FreeSurfer – BEM model

All the following instructions have to be performed in the terminal of the user's computer.
First, it is essential to activate the mne environment by introducing the command: *conda activate mne*. Then, the FreeSurfer environment needs to be setted up, this is done by following the steps 2-4 in 12.1. Finally, the BEM model is created by introducing the following command: *mne watershed_bem*. This command needs an input which is the subject name. If we use the same example as in 12.1, the final command would be: *mne watershed_bem -s SUB01.*
This command takes approximately 10-15 minutes.

## 12.3. PCA analysis results

A PCA analysis was performed over the activated sources found in encephalitic and control groups. The sources extracted were found to be activated at approximately time -0.9 (some instants before the visual stimulus were shown to the participants). The PCA results in the case of the sources found in the left hemisphere and the right hemisphere for encephalitic and control groups, respectively, did not show any concrete pattern. The results in these cases were inconclusive, since not enough participants (at least four) shared a cluster in the PCA graph.

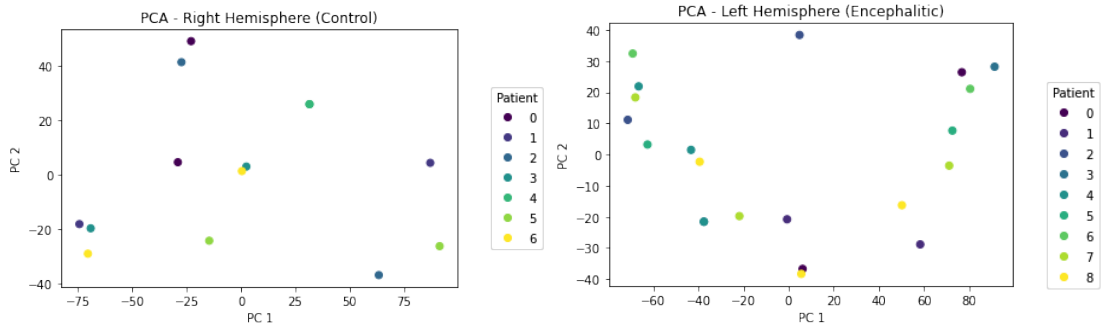


**Figure 23 and 24**: 23 and 24 depict the first two PCs and considered clusters for the source coordinates of the right and left hemispheres in Control and Encephalitic Group, respectively

## 12.4. PCA analysis code

```
# import necessary libraries
import pandas as pd
import numpy as np
import seaborn as sns
import matplotlib.pyplot as plt
import os
import numpy as np
import matplotlib.pyplot as plt
import mne
from sklearn.decomposition import PCA
import pandas as pd

control1_L1 = np.array([-9.1,-48.9,67.5])
control1_R1 = np.array([11.4,-52,65.9])
control1_L2 = np.array([-20.9,47.2,16.3])
control1_R2 = np.array([23,-57.5,22.8])

control2_L1 = np.array([-8.9,59.1,23.4])
control2_R1 = np.array([17.5,59.1,23.4])
control2_L2 = np.array([-20,33.3,42.7])
control2_R2 = np.array([11.7,-101.8,-3.4])

control3_L1 = np.array([-4.3,-46.8,46.5])
control3_R1 = np.array([48.6,35,-12.8])
control3_L2 = np.array([-7.3,-29.9,63.5])
control3_R2 = np.array([23.1,-56.8,60.3])

control4_L1 = np.array([-35.1,44.1,9.7])
control4_R1 = np.array([62,-27.7,29.5])
control4_L2 = np.array([62,-27.6,63.5])
control4_R2 = np.array([17.1,-96.8,-3.8])

control5_L1 = np.array([-26.9,54.4,16.1])
control5_R1 = np.array([19.3,2.8,44.8])
control5_L2 = np.array([-46,-63.4,25.1])
control5_R2 = np.array([19.3,2.8,44.8])

control6_L1 = np.array([-46.9,-55.9,43.4])
control6_R1 = np.array([59.7,-44,1,38.2])
control6_L2 = np.array([-5.8,54.5,-15])
control6_R2 = np.array([17.1,64.2,-7.8])
```

```
control7_L1 = np.array([-32.4,-5.6,55.2])
control7_R1 = np.array([20.7,-98,-12.6])
control7_L2 = np.array([-48.2,-81.5,12.5])
control7_R2 = np.array([62.1,-29.7,27.8])
control7_L3 =np.array([-20.1,57.2,22.6])


DATA_L =
pd.DataFrame([control1_L1,control1_L2,control2_L1,control2_L2,control3
_L1,

control3_L2,control4_L1,control4_L2,control5_L1,control5_L2,

control6_L1,control6_L2,control7_L1,control7_L2,control7_L3])

labels = [0,0,1,1,2,2,3,3,4,4,5,5,6,6,6]

pca_5 = PCA(n_components=3)
X_pca_5 = pca_5.fit_transform(DATA_L)

pca_5.explained_variance_ratio_
data= pd.DataFrame({"PC 1":X_pca_5[:,0], "PC 2":X_pca_5[:,1],"PC
3":X_pca_5[:,2]})
fig, ax = plt.subplots()
scatter=ax.scatter(x=X_pca_5[:,0],y=X_pca_5[:,1], c=labels)

legend1 = ax.legend(*scatter.legend_elements(),
title="Patient",loc='upper center', bbox_to_anchor=(1.15, 0.8))
ax.add_artist(legend1)
ax.set_xlabel("PC 1")
ax.set_ylabel("PC 2")
plt.title("PCA - Left Hemisphere (Control)")
plt.show()

import statistics
standard_dev=[]
mean = []
for index,element in enumerate(control1_L2):

    suma =
element+control2_L2[index]+control4_L1[index]+control5_L1[index]+contr
ol6_L2[index]+control7_L3[index]
    mean.append(suma/6)

standard_dev.append(statistics.stdev([element,control2_L2[index],contr
ol4_L1[index],control5_L1[index],control6_L2[index],control7_L3[index]
]))

left_control=np.round(mean,3)
print(left_control)
print(standard_dev)

DATA_R =
pd.DataFrame([control1_R1,control1_R2,control2_R1,control2_R2,control3
_R1,
```

```
control3_R2,control4_R1,control5_R1,control4_R2,control5_R2,

control6_R1,control6_R2,control7_R1,control7_R2])
labels = [0,0,1,1,2,2,3,4,3,4,5,5,6,6]

DATA_R.iloc[:,:3]
pca_5 = PCA(n_components=3)
X_pca_5 = pca_5.fit_transform(DATA_R.iloc[:,:3])

pca_5.explained_variance_ratio_
data= pd.DataFrame({"PC 1":X_pca_5[:,0], "PC 2":X_pca_5[:,1],"PC
3":X_pca_5[:,2]})

fig, ax = plt.subplots()
scatter=ax.scatter(x=X_pca_5[:,0],y=X_pca_5[:,1], c=labels)

legend1 = ax.legend(*scatter.legend_elements(),
title="Patient",loc='upper center', bbox_to_anchor=(1.15, 0.8))
ax.add_artist(legend1)
ax.set_xlabel("PC 1")
ax.set_ylabel("PC 2")
plt.title("PCA - Right Hemisphere (Control)")
plt.show()
mean=[]
for index, element in enumerate(control2_R2):
    suma = element + control4_R2[index]+control7_R1[index]
    mean.append(suma/3)
right_control=np.round(mean,3)
# analysis encefaliticos
encefalitico1_r1=np.array([19.9,27.5,37.8])
encefalitico1_r2=np.array([38.5,-66.7,1])
encefalitico1_l1=np.array([-15.3,-11.6,55.7])
encefalitico1_l2=np.array([-38.1,-88.8,-6.7])

encefalitico2_r1=np.array([20.9,-64.2,44,8])
encefalitico2_r2 = np.array([49.7,2.2,-6.5])
encefalitico2_l1 = np.array([-17.2,-64.4,51.3])
encefalitico2_l2 = np.array([-46.7,-8.1,33.8]) #CORRECT




encefalitico3_r1=np.array([23,51.2,24.7])
encefalitico3_r2 = np.array([69,-30,-14.4])
encefalitico3_l1 = np.array([-3.3,-15.8,-18.3])
encefalitico3_l2 = np.array([-14-1,61.7,1.6])
encefalitico3_r3 = np.array([37,-73.9,1.2]) #COORECT

encefalitico4_r1=np.array([32.5,-56.5,-4])
encefalitico4_r2 = np.array([41.8,-71.7,18.9])
encefalitico4_l1 = np.array([-19,-102.2,-4.2])
encefalitico4_l2 = np.array([-38,29.3,33.3])
encefalitico4_r3 = np.array([16.3,-10.7,58.5])
encefalitico4_r4 = np.array([25,54.7,-4.1])
```

```
encefalitico5_r1=np.array([36.6,7.8,-7.5])
encefalitico5_r2 = np.array([7.1,50.7,-32.6])
encefalitico5_l1 = np.array([-13.2,56.1,-8.6])
encefalitico5_l2 = np.array([-38,29.3,33.3])
encefalitico5_l3 = np.array([-45,32.6,8.4])



encefalitico6_r1=np.array([12.7,60.9,-3])
encefalitico6_r2 = np.array([49.6,-9.1,9])
encefalitico6_l1 = np.array([-15.7,-81.6,15.7])
encefalitico6_l2 = np.array([-34.4,52.4,7])
encefalitico6_r3 = np.array([13.9,9.5,-14.5])
encefalitico6_r4 = np.array([16.7,-35.4,67.6])


encefalitico7_r1=np.array([60.4,-35.4,-2.6])
encefalitico7_r2 = np.array([41.9,-75.4,11.2])
encefalitico7_l1 = np.array([-23.6,-91.1,1.4])
encefalitico7_l2 = np.array([-38.5,56.2,-23.7])
encefalitico7_r3 = np.array([44.1,-25.5,46.8]) #COORECT


encefalitico8_r1=np.array([33.7,5.8,7.2])
encefalitico8_r2 = np.array([42,-57.3,4.7])
encefalitico8_l1 = np.array([-21.4,-79.6,26])
encefalitico8_l2 = np.array([-31.2,13.9,33.8])
encefalitico8_r3 = np.array([38.7,43.5,-2.2])
encefalitico8_l3 = np.array([-9.5,58.1,-4.5])



encefalitico9_r1=np.array([28.3,-65.9,33.3])
encefalitico9r2 = np.array([44.5,29.5,20.7])
encefalitico9_l1 = np.array([-22.5,-57.7,37.1])
encefalitico9_l2 = np.array([-52.9,28.6,11.2])
encefalitico9_l3 = np.array([-35.9,-12.2,53.8])

# LEFT

DATA_L = pd.DataFrame([encefalitico1_l1,encefalitico1_l2,
                       encefalitico2_l1,encefalitico2_l2,
                      encefalitico3_l1,encefalitico3_l2,
                      encefalitico4_l1,encefalitico4_l2,

encefalitico5_l1,encefalitico5_l2,encefalitico5_l3,
                       encefalitico6_l1,encefalitico6_l2,
                       encefalitico7_l1,encefalitico7_l2,

encefalitico8_l1,encefalitico8_l2,encefalitico8_l3,

encefalitico9_l1,encefalitico9_l2,encefalitico9_l3
                      ])
```

```
labels=[0,0,1,1,2,2,3,3,4,4,4,5,5,6,6,7,7,7,8,8,8]


pca_5 = PCA(n_components=3)
X_pca_5 = pca_5.fit_transform(DATA_L)

pca_5.explained_variance_ratio_
data= pd.DataFrame({"PC 1":X_pca_5[:,0], "PC 2":X_pca_5[:,1],"PC
3":X_pca_5[:,2]})
fig, ax = plt.subplots()
scatter=ax.scatter(x=X_pca_5[:,0],y=X_pca_5[:,1], c=labels)

legend1 = ax.legend(*scatter.legend_elements(),
title="Patient",loc='upper center', bbox_to_anchor=(1.15, 0.8))
ax.add_artist(legend1)
ax.set_xlabel("PC 1")
ax.set_ylabel("PC 2")
plt.title("PCA - Left Hemisphere (Encephalitic)")
plt.show()
# RIGHT

DATA_R = pd.DataFrame([encefalitico1_r1,encefalitico1_r2,
                       encefalitico2_r1,encefalitico2_r2,

encefalitico3_r1,encefalitico3_r2,encefalitico3_r3,

encefalitico4_r1,encefalitico4_r2,encefalitico4_r3,encefalitico4_r4,
                       encefalitico5_r1,encefalitico5_r2,

encefalitico6_r1,encefalitico6_r2,encefalitico6_r3,encefalitico6_r4,

encefalitico7_r1,encefalitico7_r2,encefalitico7_r3,

encefalitico8_r1,encefalitico8_r2,encefalitico8_r3,
                       encefalitico9_r1,encefalitico9r2
                      ])

labels=[0,0,1,1,2,2,2,3,3,3,3,4,4,5,5,5,5,6,6,6,7,7,7,8,8]

pca_5 = PCA(n_components=3)
X_pca_5 = pca_5.fit_transform(DATA_R.iloc[:,:3])

pca_5.explained_variance_ratio_
data= pd.DataFrame({"PC 1":X_pca_5[:,0], "PC 2":X_pca_5[:,1],"PC
3":X_pca_5[:,2]})

fig, ax = plt.subplots()
scatter=ax.scatter(x=X_pca_5[:,0],y=X_pca_5[:,1], c=labels)

legend1 = ax.legend(*scatter.legend_elements(),
title="Patient",loc='upper center', bbox_to_anchor=(1.15, 0.8))
ax.add_artist(legend1)
ax.set_xlabel("PC 1")
ax.set_ylabel("PC 2")
plt.title("PCA - Righ Hemisphere (Encephalitic)")
plt.show()
mean=[]
```

```
standard_dev=[]
for index, element in enumerate(encefalitico1_r2):
    suma = element +
encefalitico3_r3[index]+encefalitico4_r1[index]+encefalitico7_r2[index
]+encefalitico8_r2[index]
    mean.append(suma/5)

standard_dev.append(statistics.stdev([element,encefalitico3_r3[index],
encefalitico4_r1[index],encefalitico7_r2[index],encefalitico8_r2[index
]]))
right_encefalitico=np.round(mean,3)
```

### 12.5. Source Reconstruction code

```
import numpy as np
import matplotlib.pyplot as plt
import scipy.io as sio
import pandas as pd

import mne
from mne.minimum_norm import make_inverse_operator, apply_inverse


## Define
subject = "SUB07"
subjects_dir = "/Users/anacordonavila/Desktop/Encefalitis"
mat_am =
sio.loadmat("/Users/anacordonavila/Desktop/Encefalitis/DATA_E07/EEG/S1
/E0701_single_am_longepoch.mat")
mat_pm =
sio.loadmat("/Users/anacordonavila/Desktop/Encefalitis/DATA_E07/EEG/S1
/E0701_single_pm_longepoch.mat")

trials_am = []
for element in mat_am["trial"][0]:
    trial2 = []
    for trial in element:
        #print(trial)
        electrode_before=[]
        for index, electrode in enumerate(trial):
            if index <= 1536:
                electrode_before.append(electrode)
            # record=[]
            #for recording in enumerate(electrode):
                #print(recording)
            #print(electrode)

                    # record.append(recording)
        trial2.append(electrode_before)
        #trial2.append(electrode_before)
    trials_am.append(trial2)


trials_pm = []
for element in mat_pm["trial"][0]:
    trial2 = []
```

```
    for trial in element:
        #print(trial)
        electrode_before=[]
        for index, electrode in enumerate(trial):
            if index <= 1536:
                electrode_before.append(electrode)
            # record=[]
            #for recording in enumerate(electrode):
                #print(recording)
            #print(electrode)

                    # record.append(recording)
        trial2.append(electrode_before)
        #trial2.append(electrode_before)
    trials_pm.append(trial2)
neuronav7 =
pd.read_csv('/Users/anacordonavila/Desktop/Encefalitis/DATA_E07/EEG/E0
702_Wcoord.txt',
                               skiprows=7, sep="\t")
x7 = neuronav7.iloc[0:43,3]
y7 = neuronav7.iloc[0:43,4]
z7 = neuronav7.iloc[0:43,5]


electrode_position=[]
for index,element in enumerate (x7):

electrode_position.append([float(element),float(y7[index]),float(z7[in
dex])])
electrode_position=np.asarray(electrode_position)
r7 = neuronav7.iloc[45,2:5]
n7 = neuronav7.iloc[46,2:5]
l7 = neuronav7.iloc[47,2:5]
R7 = []
N7 = []
L7 = []


for index, element in enumerate(r7):


    R7.append(float(r7[index]))
    N7.append(float(n7[index]))
    L7.append(float(l7[index]))
anatom6=[R7,N7,L7]

labels=neuronav7.iloc[0:43,0]
labels=labels.tolist()
d = dict() #dictionary keys are labels of channel and arg are position
for index, element in enumerate(electrode_position):
    d[labels[index]]=element
sampling_freq=512

## Creating MNE-Python data structures from scratch
# Create some dummy metadata
ch_types = ['eeg'] * 43
info = mne.create_info(labels,ch_types=ch_types, sfreq=sampling_freq)
```

```
trial_pm=np.array([trials_pm])
trial_am=np.array([trials_am])

creating_epochs=[]
for index,element in enumerate (trial_pm[0]):
    if index < 470:
        mean = (element+trial_am[0][index])/2
        creating_epochs.append(mean)
    else:
         creating_epochs.append(element)

simulated_epochs = mne.EpochsArray(creating_epochs, info, tmin=-
3,baseline=(-3,-1))
# defining anatomical landmarks
naison = np.array([N7[0]/1000,N7[1]/1000,N7[2]/1000])
lpa = np.array([L7[0]/1000,L7[1]/1000,L7[2]/1000])
rpa = np.array([R7[0]/1000,R7[1]/1000,R7[2]/1000])
montage = mne.channels.make_dig_montage(d,naison,lpa,rpa)
info.set_montage(montage)
montage.save("/Users/anacordonavila/Desktop/montage_E07.fif")
simulated_epochs.set_eeg_reference("average",projection=True)
noise_cov = mne.compute_covariance(
    simulated_epochs, tmax=0., method=['shrunk', 'empirical'],
rank=None, verbose=True)
fig_cov, fig_spectra = mne.viz.plot_cov(noise_cov,
simulated_epochs.info)

# CREATING EVOKED DATA
evoked = simulated_epochs.average()
evoked.plot(time_unit='s')
evoked.plot_white(noise_cov, time_unit='s')

src = mne.setup_source_space(subject, spacing='oct6',
add_dist='patch',
                             subjects_dir=subjects_dir)
## Visualization of the BEM surfaces
mne.viz.plot_bem(subject=subject, subjects_dir=subjects_dir,
                 brain_surfaces='white', orientation='coronal')
conductivity = (0.3, 0.006, 0.3)  # for three layers
model = mne.make_bem_model(subject=subject, ico=4,
                           conductivity=conductivity,
                           subjects_dir=subjects_dir)
bem = mne.make_bem_solution(model)
trans = "/Users/anacordonavila/Desktop/E07-trans.fif"
fwd = mne.make_forward_solution(info, trans=trans, src=src, bem=bem,
                                meg=False, eeg=True, mindist=5.0,
n_jobs=1,
                                verbose=True)
inverse_operator = make_inverse_operator(
    evoked.info, fwd, noise_cov, loose=0.2, depth=0.8)
method = "dSPM"
snr = 7.
lambda2 = 1. / snr ** 2
stc, residual1 = apply_inverse(evoked, inverse_operator, lambda2,
                               method=method, pick_ori=None,
```

```
                                return_residual=True, verbose=True)

method = "MNE"
stc2, residual2 = apply_inverse(evoked, inverse_operator, lambda2,
                                method=method, pick_ori=None,
                                return_residual=True, verbose=True)
method = "sLORETA"

stc3, residual3 = apply_inverse(evoked, inverse_operator, lambda2,
                                method=method, pick_ori=None,
                                return_residual=True, verbose=True)

method = "eLORETA"
stc4, residual4 = apply_inverse(evoked, inverse_operator, lambda2,
                                method=method, pick_ori=None,
                                return_residual=True, verbose=True)
vertno_max, time_max = stc.get_peak(hemi='rh')

surfer_kwargs = dict(
    hemi='both', subjects_dir=subjects_dir,
    clim=dict(kind='value', lims=[1, 5, 15]), views='lateral',
    initial_time=time_max, time_unit='s', size=(800, 800),
smoothing_steps=10)
brain =stc.plot(**surfer_kwargs)
brain.add_foci(vertno_max, coords_as_verts=True, hemi='lh',
color='blue',
               scale_factor=0.6, alpha=0.5)
brain.add_text(0.1, 0.9, 'dSPM (plus location of maximal activation)',
'title',
               font_size=14)
```